Journal of Organometallic Chemistry 886 (2019) 13–26

Contents lists available at ScienceDirect

Journal of Organometallic Chemistry

journal homepage: www.elsevier.com/locate/jorganchem

Cyclooctadiene iridium complexes with phosphine and pentadienyl ligands☆

Amira Reyna-Madrigal, Naytzé Ortiz-Pastrana, M. Angeles Paz-Sandoval*

Departamento de Química, Centro de Investigación y de Estudios Avanzados del IPN, Av. IPN # 2508, San Pedro Zacatenco, Ciudad de México, 07360, Mexico

ARTICLE INFO

Article history:
Received 19 December 2018
Received in revised form
4 February 2019
Accepted 5 February 2019
Available online 15 February 2019

Keywords:
Iridium
Pentadienyl
Cyclooctadiene
Phosphine

ABSTRACT

Reaction of $[(\eta^4\text{-COD})Ir(\mu_2\text{-Cl})]_2$ (**1**) with tin $CH_2CRCHCRCH_2SnR'_3$ (R = H, Me; R' = Me, *n*-Bu) or lithium pentadienide reagents gives the corresponding acyclic pentadienyl sandwich compounds $[(\eta^4\text{-COD})Ir(\eta^5\text{-}CH_2CMeCHCMeCH_2)]$ (**2**) and $[(\eta^4\text{-COD})Ir(\eta^5\text{-}CH_2CHCHCHCH_2)]$ (**3**). Treatment of **1** with different phosphines affords the well-known mononuclear phosphine complexes $[(\eta^4\text{-COD})IrClPR_3]$ [R = Ph, **4**; *i*-Pr, **5**; Me, **6**] which react with lithium pentadienide to give the exclusive formation of $[(\eta^4\text{-COD})Ir(1\text{-}3\text{-}\eta\text{-}CH_2CHCHCHCH_2)PR_3]$ [R = Ph, **7**; P(*i*-Pr), **8**], whereas the less steric trimethylphosphine shows an equilibrium mixture of the *pseudo* iridacyclic $[(\eta^4\text{-COD})Ir(1,4\text{-}5'\text{-}\eta\text{-}CH_2CHCHCHCH_2)PMe_3]$ (**9a**) and $[(\eta^4\text{-COD})Ir(1\text{-}3\text{-}\eta\text{-}CH_2CHCHCHCH_2)PMe_3]$ (**9b**) in a 2:1 ratio. Additionally, the addition reaction of phosphines to compound **2** gives the dimethyl-pentadienyl complexes $[(\eta^4\text{-COD})Ir(1\text{-}3\text{-}\eta\text{-}CH_2CMeCHCMeCH_2)PPh_3]$ (**10**) and the mixture of isomers $[(\eta^4\text{-COD})Ir(1,4\text{-}5'\text{-}\eta\text{-}CH_2CMeCHCMeCH_2)PMe_3]$ (**11a**) and $[(\eta^4\text{-COD})Ir(1\text{-}3\text{-}\eta\text{-}CH_2CMeCHCMeCH_2)PMe_3]$ (**11b**) in a 2:1 ratio. Compounds **2**, **4**, **5**, **6**, **7**, **8**, **9b**, **10** and **11a** have been structurally characterized by single-crystal X-ray diffraction studies. The influence of the electronic and steric effects of the different ligands, as well as the preference of the bonding modes in the pentadienyl ligands is analyzed and contrasting to pentadienyl electron rich complexes, derived from $IrCl(PR_3)_3$, previously described in the literature.

1. Introduction

The cycloocta-1,5-diene ligand (COD) is a popular ancillary ligand in iridium chemistry, with a great number of accessible compounds and common starting materials [1]. As a result of the accessibility of $[(\eta^4\text{-COD})Ir(\mu\text{-Cl})]_2$ (**1**) [2], iridium cyclooctadiene complexes with interesting properties have been reported [1c,3] and many of them have been useful in various homogeneous catalytic reactions [1c,4].

In previous years, a versatile and interesting chemistry with heteronuclear substituents in acyclic unsaturated ligands (pentadienyl analogues in which one terminal CH_2 group has been replaced by heteroatoms, such as oxygen, sulfur or sulfur dioxide) has been described which included the $(\eta^4\text{-COD})Ir$ moiety [3b,5-7].

These results motivated further research on the acyclic unsaturated pentadienyl ligands, as well as the influence of tertiary phosphines in the preference of bonding modes, when they are coordinated to the iridium cyclooctadiene moiety.

Previously, the reactions of allylic complexes, such as $(\eta^4\text{-COD})Ir(\eta^3\text{-}C_3H_4X)$ (X = H, Me) with various types of phosphites have been examined and published elsewhere [8]. In particular, the reaction of allyllithium and dimer **1** yielded $[(\eta^4\text{-COD})Ir(\eta^3\text{-allyl})]$ a thermally reactive molecule [8,9], which can react with trimethylphosphite, yielding the corresponding $[(\eta^4\text{-COD})Ir(\eta^3\text{-allyl})(\text{-}P(OMe)_3)]$ or $[(\eta^4\text{-COD})Ir(\eta^1\text{-allyl})(P(OMe)_3)_2]$, where the former is a catalysis for olefin hydrogenation [9].

A systematic study by Bleeke et al. regarding the reactions of electron rich complexes $IrCl(PR_3)_3$ (R = Et, Me) [10,11], ½ $[IrCl(\text{-}PEt_3)_2]_2$ [12], as well as Vaska's derivatives from $Ir(Cl)(CO)(PR_3)_2$ (R = Et, Ph) [11] with lithium pentadienide and 2,4-dimethyl-pentadienide reagents have shown to produce 1-3-η-pentadienyl, 1,4-5-η-pentadienyl and 1,5-η-iridacyclohexa-2,4-diene complexes or equilibrium mixtures as summarized in Scheme 1 [10–13] and 2 [11], respectively.

In contrast to the pentadienyl iridium chemistry of electron-rich complexes and Vaska's derivatives shown in Schemes 1 and 2, respectively, the present study describes the results of the

☆ *In memoria* of Professor Pascual Royo leadership in the field of organometallic chemistry.

* Corresponding author.
E-mail address: mpaz@cinvestav.mx (M.A. Paz-Sandoval).

https://doi.org/10.1016/j.jorganchem.2019.02.007
0022-328X/

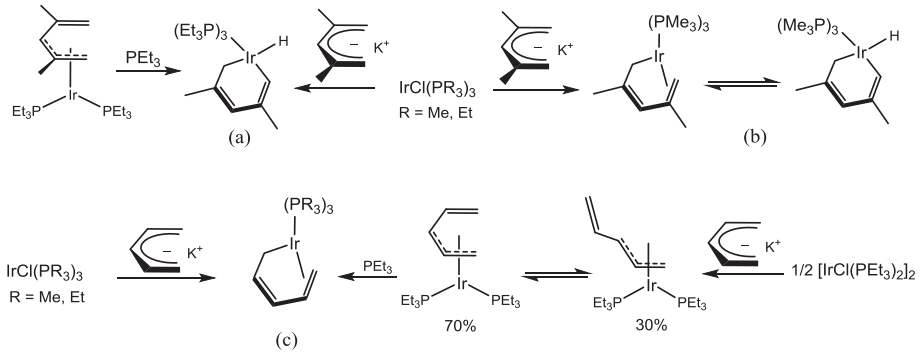

Scheme 1. Influence of the substituents on the pentadienyl and phosphine ligands in electron rich complexes [10–13].

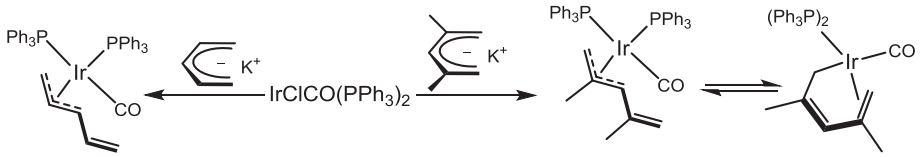

Scheme 2. Reactivity of Vaska's complex with pentadienide salts [11].

pentadienyl iridium chemistry which involves less electron-rich ligands, such as the reactivity of dinuclear iridium cyclooctadiene complex **1**, as well as mononuclear phosphine complexes (η^4-COD)Ir(PR_3) [R = Ph, (**4**) *i*-Pr, (**5**) Me (**6**)] toward lithium pentadienide, 2,4-dimethylpentadienide or tin-pentadiene reagents. The influence of the electronic and steric effects of the complementary ligands involved in the pentadienyl compounds will be analized.

2. Results and discussion

2.1. Pentadienyl chemistry

Reaction of [(η^4-COD)Ir(μ_2-Cl)]$_2$ (**1**) with 2,4-dimethyl-1-trimethyltin-2,4-pentadiene reagent led to the formation of [(η^4-COD)Ir(2,4-dimethyl-η^5-pentadienyl) (**2**) in 90% yield, (Scheme 3). The synthesis of the [(η^4-COD)Ir(η^5-pentadienyl) (**3**) was carried out through the transmetallation and metathesis reactions with the 1-tributyltin-2,4-pentadiene or lithium pentadienide prepared *in situ* at −78 °C from 1,4-pentadiene and lithium di*iso*propylamine (LDA) in THF, (Scheme 3).

The high volatility and solubility, as well as the thermal instability of compound **3**, allowed to obtain only the spectroscopic characterization through the ^{1}H and ^{13}C NMR. In contrast, compound **2** was isolated as a stable yellow solid and fully characterized. It has been known that the presence of methyl groups substituted in pentadienyl ligands confers higher stability to the complexes which contain them, and there is also a preference of the U conformer if the methyl substitution occurs on C2 and C4 [14], see Scheme 3.

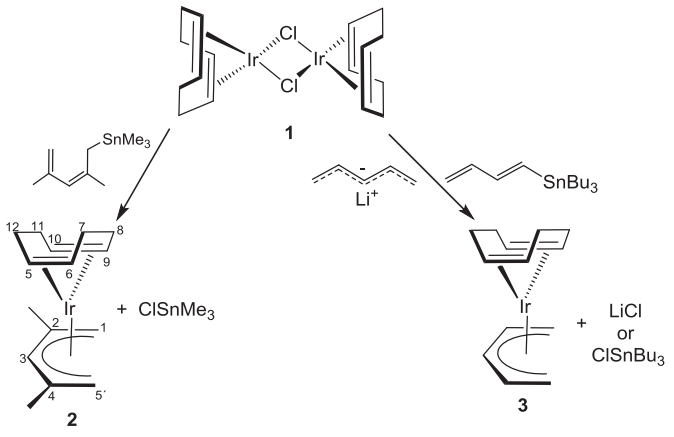

Scheme 3. Trasmetallation and metathesis reactions of compounds **2** and **3**.

The ^{1}H and ^{13}C NMR data of compounds **2** and **3** are described in Tables 1 and 2, respectively. The ^{1}H NMR of **2** shows all chemical shifts as broad bands, in C_6D_6, at room temperature. Further support for the full assignment of **2** was obtained by ^{1}H and ^{13}C NMR in CD_2Cl_2 at −90 °C, as well as by the coupled ^{13}C NMR. The assignment is consistent with a *U* conformation for the pentadienyl ligand. Similar chemical shifts have been observed for related complexes [(η^5-C_5H_5)Ir(2,4-dimethyl-η^5-pentadienyl)]$^+$ and [(2,4-dimethyl-η^5-pentadienyl)Ir(η^4-CH_2CMeCHC(Me)$_2$)] [15]. At room temperature the CH and CH_2 carbon and hydrogen of the COD ligand in **2** are equivalent between each other. However, at low temperature, there is no magnetic equivalence and all hydrogen and carbon atoms can be assigned. Compound **3** has been assigned based on compound **2**. The molecular structure of **2** has been obtained from a single-crystal X-ray diffraction study. The crystalline structure is shown in Fig. 1, crystal data, bond lengths and angles are described in Tables 4 and 6, respectively.

The iridium atom in **2** is within bonding distances of the four olefinic carbon atoms of the COD, and five carbon atoms of the 2,4-dimethyl-η^5-pentadienyl ligands. These bond lengths are in the range of 2.092(6) to 2.167(5) and 2.141(8) to 2.284(5) Å, respectively.

The iridium bond lengths with the non-conjugated olefin carbon atoms are shorter for C5 (2.112(5) Å) and C6 (2.092(6) Å) and longer for C9 (2.167(5) Å) and C10 (2.158(8) Å), while the double bond C5-C6 (1.442(9) Å) is longer than C9-C10 (1.401(8) Å). The elongation of the COD double bonds is consistent with back donation to the π^* orbitals from a low valent Ir(I). The elongation is not symmetric, with C5-C6 being larger than C9-C10, similar than those for five coordinate geometries, such as (η^4-COD)$_2$IrCl [16], (η^4-COD)Ir(1-2,5-η-butadienesulfonyl)(L) (L = PMe_3, PMe_2Ph, PPh_3, CO, DMSO) [5], (η^4-COD)Ir(5-η-butadienesulfonyl)(PMe_3)$_2$

Table 1
1H NMR[a] of compounds **2-8**, **9a**, **9b**, **10**, **11a** and **11b**.

Pentadienyl							COD								PR_3	^{31}P {^1H}
Compound	$H1_{anti}/H5_{anti}$	$H1_{syn}/H5_{syn}$	H2/Me	H3	H4/Me	H5'/H5'	H5	H6	H7	H8	H9	H10	H11	H12		
2[b]	1.44	2.80	1.70	5.53	1.70		3.39	3.39	2.23	2.23	3.39	3.39	2.23	2.23		
2[b,c]	0.57 1.66	1.93 3.30	2.17	5.90	1.51	2	2.25	4.01	2.46 3.13	1.18 1.85	2.33	4.01	~1.50 2.17	1.35 1.85		
3[d]	1.32 (d, 8.7)	2.83 (dd, 2.2, 8.4)	4.60 (m, 8.4)	5.49 (t, 6.1)	4.60 (m, 8.4)		3.54	3.54	2.21	2.21	3.54	3.54	2.21	2.21		
4[d]							2.83	2.83	1.60 (m, 8.0) 2.07 (m, 5.6)	1.39 (m, 7.6) 2.07 (m, 5.6)	5.53	5.53	1.39 (m, 7.6) 2.07 (m, 5.6)	1.60 (m, 8.0) 2.07 (m, 5.6)	7.03 7.84 (m, 8.2)	22.5
5	P(i-Pr)3						3.06 (q,ap, 2.8)	3.06 (q,ap, 2.8)	1.51 (m) 2.06−2.16 (m)	1.51 (m) 1.93−2.05 (m)	5.24 (q,ap, 2.8)	5.24 (q,ap, 2.8)	1.51 (m) 1.93−2.05 (m)	1.51 (m) 2.06−2.16 (m)	1.11 (d, 7.2) 1.15 (d, 7.2) 2.33 (m)	25.7
5[e]	P(i-Pr)3						3.27 (q,ap, 2.4)	3.27 (q,ap, 2.4)	1.70 (m) 2.17 (m)	1.60 (m) 2.17 (m)	4.84 (m)	4.84 (m)	1.60 (m) 2.17 (m)	1.70 (m) 2.17 (m)	1.32 (d, 7.2 1.36 (d, 7.2) 2.54 (m, 7.4, 8.9)	26.5
6							2.90 (q,ap, 3.3)	2.90 (q,ap, 3.3)	1.62 2.03	1.55 2.15	5.28 (q,ap, 2.4)	5.28 (q,ap, 2.4)	1.55 2.15	1.62 2.03	0.97 (d, 9.6)	−15.5
6[d,e]							3.14 (q,ap, 3.2)	3.14 (q,ap, 3.2)	1.68 1.84	1.46 2.20	4.97 (q,ap, 2.8)	4.97 (q,ap, 2.8)	1.46 2.20	1.68 1.84	1.40 (d, 10.4)	−14.6
7[d]	0.44 (dd, br, 5.9, 12.4)	1.60[f] (br)	4.87 (m)	2.99 (dt, 9.9, 13.0)	6.20 (dt, 10.1, 16.8)	5.16 (d, 17.1) 5.25 (d, 10.1)	3.62	2.55	1.22−1.93	1.22−1.93	3.81	3.81	2.30	1.00−1.50	7.45 (t, 8.5, *o*) 6.90−7.11 (m, *m*,*p*)	10.2
8[d]	1.28 (t, 7.6)	~2.21[f]	4.69 (m)	3.45 (q,ap, 10.0)	6.15 (dt, 10.7, 16.6)	5.17 (d, 6.7) 5.20 (s)	2.94	2.94	2.06−2.26	1.97	3.70	3.70	1.98−2.30	1.98−2.30	0.99 (d, 7.2) 1.03 (d, 7.2) 2.10 (sept, 7.2)	5.28
9a	0.77 (H1) (d, br, 16.1)	1.31 (H1′) (d, br, ~16.0)	5.64 (m)	6.36 (m, br)	4.18 (m, br)	1.20−1.50 (m) 1.80−2.60 (m)	3.02 (m)	2.50 (m)	2.24 (m)	2.10 (m)	2.31 (m)	3.44 (m)	2.04 (m) 2.40 (m)	2.78 (m)	1.08 (d, 8.2)	−53.7
9b	1.42 (dd, 12.6, 7.9)	1.54 (dd, 4.2, 7.4)	4.95[f]	2.40[f]	6.05 (dt, 10.1, 17.1)	4.86−5.04 (m)	3.02 (m)	2.50 (m)	2.24 (m)	2.10 (m)	2.31 (m)	3.44 (m)	2.04 (m) 2.40 (m)	2.78 (m)	0.99 (d, 7.7)	−52.7
10[d]	0.61 (d, 22.8)	1.99	2.65 (d, 5.7)	1.90	1.77 (s)	5.18 (s) 5.28 (s)	3.28	3.65	1.55 1.20−2.40	2.32 2.10−2.40	3.53	3.80	1.44 1.20−2.10	1.84 1.35−2.40	7.48 (t, 7.7, *o*) 7.05−7.16 (m, *m*,*p*)	10.7
11a	0.67 (d, 16.1)	1.13 (t, 16.6)	2.29 (d, 7.0)	5.91 (br, 3.3)	1.85 (s)	1.43 (d, 2.5) 2.28[f] (m)	3.25 (m)	1.64−2.34 (m)	2.52 (m) 2.70 (m)	1.33 (m) 1.64−2.34 (m)	2.70 (m)	3.44 (m)	1.64−2.34 (m)	1.64−2.34 (m)	1.06 (d, 7.8)	−52.4 −58.5[c] −50.3[g]
11b	0.47 (d, 25.2)	1.10[f]	2.78 (d, 6.6)	2.25[f]	1.54 (s)	5.12 (s) 5.34 (s)	3.13 (m)	3.32 (m)	2.00 (m) 2.52 (m)	2.10 (m) 2.23 (m)	3.12 (m)	3.12 (m)	1.91 (m) 2.30 (m)	1.63 (m) 2.23 (m)	0.95 (d, 7.4)	−55.5 −59.3[c] −60.5[g]
11a[e]	0.37 (d, 16.3)	1.01 (t, 16.3)	2.02 (d, 7.2)	5.54 (s,br)	1.59 (s)	1.27 (m) 2.72[f]	3.50 (m)	3.29 (s,br)	2.11 (m)	1.34 (m) ~1.50 (m)	2.60 (m)	2.83 (m)	2.11 (m)	1.56 (m)	1.49 (d, 8.2)	−50.7
11b[e]	0.32 (d, 25.2)	1.20−1.60[f]	2.60 (d, 6.4)	2.20[f]	1.92 (s)	4.85 (s) 5.02 (s)	2.93 (m)	3.19 (m)	2.10−2.30 2.60 (m)	2.10−2.30 (m)	2.83 (m)	2.83 (m)	1.20−1.60 (m) 2.10−2.30 (m)	1.20−1.60 (m) 2.10−2.30 (m)	1.41 (d, 7.4)	−53.4

a) In C_6D_6. δ in ppm and *J* in hertz. For numbering see Schemes 3-5.
b) All chemical shifts appear as broad singlets (except where otherwise stated).
c) In CD_2Cl_2 at −90 °C.
d) All COD signals appear broad (except where otherwise stated).
e) In $CDCl_3$.
f) Overlapped signals.

Table 2
$^{13}C\{^{1}H\}$ NMR[a] of compounds **2-8**, **9a**, **9b**, **10**, **11a**, **11b** and **11c**.

Compound	Pentadienyl					COD								PR_3
	C1	C2/Me	C3	C4/Me	C5′	C5	C6	C7	C8	C9	C10	C11	C12	
2	44.1	101.7 23.7	100.1	101.7 23.7	44.1	56.0 (br)	56.0 (br)	34.3	34.3	56.0 (br)	56.0 (br)	34.3	34.3	
2[b]	44.1 (t, 156.2)	101.7 23.7 (q, 127.2)	100.1 (d, 161.0)	101.7 23.7 (q, 127.2)	44.1 (t, 156.2)	55.7 (d, 148.4)	55.7 (d, 148.4)	34.3 (t, 125.1)	34.3 (t, 125.1)	55.7 (d, 148.4)	55.7 (d, 148.4)	34.3 (t, 125.1)	34.3 (t, 125.1)	
2[c]	43.1	103.0 25.3	100.4	101.2 23.0	42.1	53.3	45.6	42.2	26.6	64.1	58.6	36.8	30.4	
3	41.7	89.8	101.2	89.8	41.7	55.5 (br)	55.5 (br)	34.7	34.7	55.5 (br)	55.5 (br)	34.7	34.7	
4						52.9 (s)	52.9 (s)	33.5 (s)	29.6 (s)	94.1 (d, 14.3)	94.1 (d, 14.3)	29.6 (s)	33.5 (s)	135.2 (d, 11.0, *o*) 131.4 (d, 49.5, *i*) 130.1 (d, 1.9, *p*) 127.9 (d, 9.5, *m*)
5						50.7 (s)	50.7 (s)	33.8 (d, 2.6)	29.0 (d, 1.7)	90.5 (d, 13.5)	90.5 (d, 13.5)	29.0 (d, 1.7)	33.8 (d, 2.6)	19.6 (s) 22.6 (d, 24.4)
5[d]						51.5 (s)	51.5 (s)	33.7 (d, 2.9)	28.8 (d, 1.7)	90.3 (d, 13.3)	90.3 (d, 13.3)	28.8 (d, 1.7)	33.7 (d, 2.9)	19.9 (s) 22.6 (d, 24.4)
6						49.6 (s)	49.6 (s)	34.0 (d, 2.9)	29.2 (s)	92.7 (d, 15.4)	92.7 (d, 15.4)	29.2 (s)	34.0 (d, 2.9)	12.0 (d, 33.6)
6[d]						51.3 (s)	51.3 (s)	29.1 (s)	33.9 (d, 3.3)	93.3 (d, 14.8)	93.3 (d, 14.8)	33.9 (d, 3.3)	29.1 (s)	12.8 (d, 33.6)
7	32.3 (d, 4.7)	73.8 (d, 4.7)	60.1	141.8 (d,1.6)	109.2	58.9 (d, br, 20.2)	50.3 (br)	39.2 (br)	28.6 (br)	75.0 (br)	66.7 (br)	36.5 (br)	30.2 (br)	137.1 (d, 35.8, C*i*) 134.4 (d, 10.4, *o*) 128.2[e] (*m*) 129.2 (s, *p*)
8	24.4 (d, 4.8)	70.8 (d, ~4.0)	54.6 (d, ~4.0)	141.6	107.5	51.2	51.2	34.3	34.3	66.5	66.5	34.3	34.3	19.9 (Me) 27.6 (d,14.4)
9a	17.9 (d, 9.3)	136.8 (d, 12.5)	138.3 (d, 4.7)	56.1 (d, 15.6)	25.9 (d, 6.2)	59.9 (d,15.6)	58.9 (d, 7.3)	33.6 (d, 4.7)	34.1 (d, 2.1)	89.2 (d, 4.2)	74.9 (d, 3.6)	32.2 (d, 2.6)	37.3	16.4 (d, 28.0)
9b	34.6 (d, 8.3)	64.3 (d, 5.7)	52.7 (d, 5.2)	142.6	107.5	59.9 (d,15.6)	58.9 (d, 7.3)	33.6 (d, 4.7)	34.1 (d, 2.1)	89.2 (d, 4.2)	74.9 (d, 3.6)	32.2 (d, 2.6)	37.3	17.4 (d, 25.0)
10	37.4 (d, 6.5)	80.3 (d, 5.1) 20.9	57.1 (d, 4.1)	145.3 26.1	109.3	61.4 (d, 19.3)	56.1	33.6	34.3	73.7	62.6	30.9	32.6	136.2 (d, 33.7, C*i*) 134.2 (d, 10.1, *o*) 128.9 (s, *p*) 128.0[e] (*m*)
11a	21.6 (d, 9.1)	141.1 (d, 8.4) 21.0	138.3 (d, 2.9)	63.0 (d, 17.2) 25.7	29.7 (d, 3.3)	60.5 (d, 17.8)	50.4 (d, 5.7)	39.5 (d, 8.6)	28.4	84.3 (d, 4.5)	74.1 (d, 2.8)	38.5	37.1	15.4 (d, 27.8)
11a[d]	21.2 (d, 10.4)	141.8 20.9	137.6	n.o.[f] 25.4	29.6	60.1 (d, 17.7)	55.1 (d, 6.8)	43.4	28.3	84.5	74.4	38.2	34.1	16.1 (d, 28.0)
11a[g]	21.2 (d, 9.3)	141.6 (d, 8.4) 20.7	137.7	61.8 (d,16.9) 25.2	29.4 (d,<3.0)	59.7 (d, 17.7)	54.9 (d, 6.9)	43.2	28.1	84.1 (d, 3.9)	74.5 (d,3.1)	38.3	34.0 (br)	15.7 (d, 28.4)
11b	31.9 (d, 7.3)	71.1 (d, 6.3) 21.5	55.2 (d, 6.8)	145.7 26.4	107.1	57.0 (d, 5.4)	53.7 (d, 5.7)	33.2	32.5	70.4 (d, 13.1)	61.6 (d, 17.7)	35.0	34.4	17.0 (d, 24.0)
11b[d]	31.6 (d, ~9.3)	n.o[f] 21.3	55.9 (s, br)	143.0 26.4	106.5	56.9 (d,~5.0)	53.8 (d~5.0)	32.9	32.3	70.3 (d, 12.5)	61.5 (d, ~15.0)	36.9	34.9	17.7 (d, 24.3)
11c[h,i,j]	32.7 (d, 6.9)	102.1 25.0	55.6 (d, 5.3)	149.1 (d, 12.3) 25.9	100.3	65.2 (d, 17.7)	52.1 (m, 3.8)	30.8	29.3	70.5 (d, 6.2)	67.3 (d, 13.9)	37.0	36.9	16.2 (d, 24.6)

[a] In C_6D_6. δ in ppm, *J* in hertz. For numbering see Schemes 3-5.
[b] Coupled spectrum.
[c] In CD_2Cl_2 at −90 °C.
[d] In $CDCl_3$.
[e] Overlapped signals.
[f] Not observed.
[g] In CD_2Cl_2 at 0 °C.
[h] In CD_2Cl_2 at −40 °C.
[i] Tentative assignment for COD signals.
[j] ^{31}P δ = −47.7.

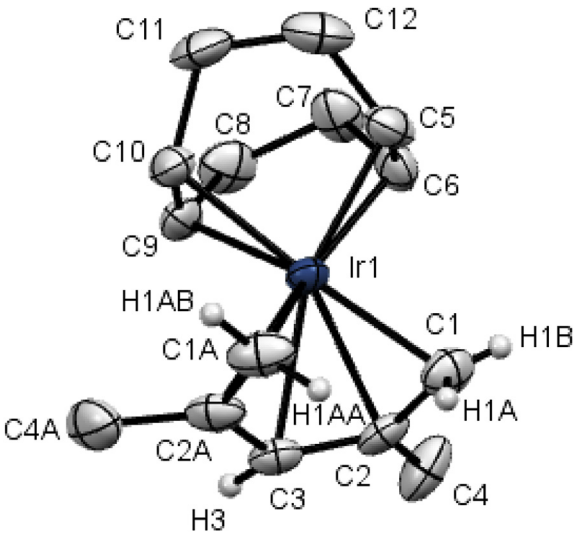

Fig. 1. Molecular structure of compound [(η^4-COD)Ir(2,4-dimethyl-η^5-pentadienyl) (**2**). Hydrogen atoms have been omitted for the sake of clarity, except those of the pentadienyl ligand.

[5], as well as compounds **7**, **8**, **9b**, **10**, **11a**, described here, *vide infra*. The asymmetric bond lengths of the coordinated carbon atoms of the COD ligand in compound **2** are contrasting with those of symmetric elongations in compounds [(η^4-COD)Ir(η^5-C_5H_5)Br]PF_6 [17a], [(η^4-COD)Ir(η^5-C_5H_4)CMe_2(η^5-C_9H_6)$_2$Ir(η^4-COD)] [17b], [(η^4-COD)Ir(η^5-C_5H_4Me)] [17c], and [(η^4-COD)Ir(η^5-C_5Me_5)] [17d].

The iridium bond length of the terminal carbon atom C1 (2.141(8) Å) of the pentadienyl ligand is significantly shorter than C1A (2.266(6) Å), while the internal carbon atoms are quite symmetric (C2, 2.240(5), C2A, 2.235(6) Å) and the longest bond length is found for the central carbon atom C3 (2.284(5) Å).

Atoms C1, C2, C3, C2A, and C1A of the 2,4-dimethylpentadienyl ligand are planar to within 1.80°. Methyl carbon atoms C4 and C4A are displaced out of the plane toward the iridium atom by 0.197 and 0.331 Å**,** respectively. These bending displacements have been previously observed in similar compounds, and it has been explained as a result of a better overlap with the appropriate metal orbitals [18]. The C-C-C angles within the iridium-bound portion of the pentadienyl ligand are near and expanded somewhat from the ideal of 120° (119.1(6), 126.9(5), and 124.2(6) for angles C1-C2-C3, C2-C3-C2A, and C3-C2A-C1A, respectively).

2.2. Pentadienyl phosphine chemistry

2.2.1. Pentadienyl complexes

Compounds [(η^4-COD)IrClPR$_3$] [R = Ph, **4**; [2a,2e,5] *i*-Pr, **5** [2e]; Me, **6** [5]] used in this study are known. However, in this report, we describe an alternative synthetic procedure for compounds **5** and **6**, and the full characterization of **5**. The chemistry of **4**–**6** with the lithium pentadienide salt is summarized in Scheme 4.

The higher cone angles of the phosphine ligands in **4** (145°) [19a] and **5** (160°) [19b,c] afford the exclusive formation of [(η^4-COD)Ir(1-3-η-$CH_2CHCHCHCH_2$)PR_3] [R = Ph, **7**, 89%; P(*i*-Pr), **8**, 33%]. Whereas the less steric trimethylphosphine (118°) [19a] shows an equilibrium mixture of isomers in 60% yield: the *pseudo* iridacyclic [(η^4-COD)Ir(1,4-5′-η-$CH_2CHCHCHCH_2$)PMe_3] (**9a**) and [(η^4-COD) Ir(1-3-η-$CH_2CHCHCHCH_2$)PMe_3] (**9b**) in a 2:1 ratio [20].

The reactions proceed immediately for **7** and **8** at −110 °C, changing from strong-orange to yellow, while a slower reaction (12 h), at room temperature, was observed for **9a** and **9b**. Comparative NMR spectroscopic data for complexes **7**, **8**, **9a** and **9b** are summarized in Tables 1 and 2

For the 1-3-η-pentadienyl coordination there are two classical bonding modes [14b]: the first and by far most common mode is directly analogous to that of a typical η^3-allyl complex, observed for **7**, **8** and **9b**; and the second involving localization of the dienyl fragment, and formation of formal metal-alkyl and metal-olefin interactions, such as **9a**, common in some iridium compounds [11,12].

In compounds **7**, **8** and **9b** the pronounced high frequency chemical shift of H5′ and H5′′ (4.86–5.25) observed for the η^3-coordinated pentadienyl ligand reflects the non-coordination of the terminal double bond. The protons H2 and H3 resonate at δ 4.69–4.98 and 2.40–3.45, respectively, while the terminal $H1_{anti}$

Table 3
Crystal Data for compounds **4**, **5** and **6**.

formula	4	5	6
	C_{27} H_{28} Cl_4 Ir P	C_{17} H_{33} Cl Ir P	C_{11} H_{21} Cl Ir P
mol wt	717.46	496.05	411.90
space group	$P2_1/m$	$P2_1/c$	$P2_1/c$
a (Å)	9.820(2)	7.9318(8)	6.8595(4)
b (Å)	12.146(2)	16.0902(18)	11.4387(7)
c (Å)	11.606(2)	14.8584(16)	16.8676(10)
α (deg)	90.00	90.00	90.00
β (deg)	98.35(3)	99.731(3)	101.197(2)
γ (deg)	90.00	90.00	90.00
V (Å^3)	1369.7(5)	1869.0(3)	1298.30(13)
Z	2	4	4
Cryst size (mm)	0.15 × 0.09 × 0.05	0.300 × 0.085 × 0.060	0.282 × 0.140 × 0.066
Dcalc (g cm^{-3})	1.740	1.763	2.107
Temperature K	293(2)	298(2)	150(2)
θ limit (deg)	1.773–28.694	2.532–29.522	2.462–30.507
h, k, l ranges	−13 ≤ h ≤ 13	−10 ≤ h ≤ 10	−9 ≤ h ≤ 9
	−16 ≤ k ≤ 16	−22 ≤ k ≤ 22	−16 ≤ k ≤ 16
	−15 ≤ l ≤ 15	−20 ≤ l ≤ 20	−24 ≤ l ≤ 24
total no. data	7067	128269	40007
total no. unique data	3694 [R(int) = 0.0180]	4961 [R(int) = 0.0287]	3940 [R(int) = 0.0313]
Final R indices [I > 2sigma (I)]	0.0216	0.0184	0.0155
final *w*R2	0.0567	0.0404	0.0407
GOF	1.134	1.163	1.074

Table 4
Crystal data for pentadienyl compounds **2**, **7**, **8**, **9b**, **10**, and **11a**.

formula	2	7	8	9b	10	11a
	C_{15} H_{23} Ir	C_{31} H_{34} Ir P	C_{22} H_{40} Ir P	C_{16} H_{28} Ir P	C_{33} H_{38} Ir P	C_{18} H_{32} Ir P
mol wt	395.53	629.75	527.71	443.55	657.80	470.60
space group	$P2_1/n$	Pnaa	$P2_1/n$	$P2_1/c$	$Pca2_1$	C2/c
a (Å)	7.6780(3)	8.3267(2)	9.23280(10)	9.0360(2)	8.3193(17)	17.5475(8)
b (Å)	11.5620(4)	17.4396(6)	13.8401(2)	15.0192(3)	18.205(4)	8.5211(3)
c (Å)	15.0440(5)	35.8607(13)	17.2953(2)	12.7658(2)	35.601(7)	24.1519(10)
α (deg)	90.00	90.00	90.00	90.00	90.00	90.00
β (deg)	95.141(2)	90.00	102.3170(10)	110.4710(10)	90.00	96.115(2)
γ (deg)	90.00	90.00	90.00	90.00	90.00	90.00
V ($Å^3$)	1330.13(8)	5207.5(3)	2159.17(5)	1623.08(6)	5391.8(19)	3590.7(3)
Z	4	8	4	4	8	8
Cryst size (mm)	0.29 × 0.15 × 0.10	0.19 × 0.11 × 0.08	0.2 × 0.2 × 0.1	0.3 × 0.15 × 0.08	0.12 × 0.07 × 0.05	0.18 × 0.10 × 0.08
Dcalc (gcm^{-3})	1.975	1.606	1.620	1.815	1.621	1.741
Temperature K	293(2)	293(2)	293(2)	293(2)	173(2)	173(2)
θ limit (deg)	3.564–27.466	3.202–27.509	0.7456–0.5389	3.627–27.488	3.317–27.517	3.088–27.331
h, *k*, *l* ranges	$-8 \le h \le 9$	$-9 \le h \le 10$	$-11 \le h \le 9$	$-11 \le h \le 11$	$-9 \le h \le 10$	$-22 \le h \le 22$
	$-13 \le k \le 14$	$-22 \le k \le 22$	$-17 \le k \le 17$	$-19 \le k \le 19$	$-23 \le k \le 23$	$-9 \le k \le 10$
	$-19 \le l \le 19$	$-20 \le l \le 46$	$-22 \le l \le 21$	$-14 \le l \le 16$	$-46 \le l \le 46$	$-19 \le l \le 31$
total no. data	7980	27614	31708	18969	16388	10143
total no. unique data	2953 [R(int) = 0.0448]	5862 [R(int) = 0.0861]	4919 [R(int) = 0.1119]	3710 [R(int) = 0.0347]	9155 [R(int) = 0.0298]	3906 [R(int) = 0.0451]
Final R indices [I > 2sigma (I)]	0.0346	0.0456	0.0291	0.0228	0.0283	0.0372
final *w*R2	0.0891	0.1114	0.0739	0.0531	0.0614	0.0727
GOF	1.055	1.041	1.039	1.045	1.033	1.097

Table 5
Selected bond lengths (Å) and angles (°) of compounds **4**, **5** and **6**.

Bond lengths (Å)			
	4	5	6
Ir1-C5	2.112(3)	2.113(2)	2.101(2)
Ir1-C6	2.112(3)	2.141(2)	2.1044(19)
Ir1-C9	2.180(3)	2.195(2)	2.182(2)
Ir1-C10	2.180(3)	2.191(2)	2.214(2)
Ir1-Cl1	2.3558(12)	2.3668(6)	2.3538(5)
Ir1-P1	2.3172(9)	2.3522(5)	2.2993(5)
C5-C6	1.430(8)	1.428(3)	1.433(3)
C9-C10	1.389(11)	1.394(3)	1.396(3)
Bond Angles (°)			
	4	**5**	**6**
C(5)-Ir(1)-P(1)	94.5(9)	93.4(7)	93.2(6)
C(6)-Ir(1)-P(1)	94.5(9)	98.4(6)	95.4(6)
C(9)-Ir(1)-Cl(1)	87.9(11)	87.4(7)	88.6 (6)
C(10)-Ir(1)-Cl(1)	87.9(11)	87.3(7)	93.6(6)
P(1)-Ir(1)-Cl(1)	90.5(5)	90.1(2)	87.3(2)
C(5)-Ir(1)-Cl(1)	159.6(11)	154.6 (7)	160.7(7)
C(6)-Ir(1)-Cl(1)	159.6(11)	163.7(7)	159.4(6)
C(9)-Ir(1)-P(1)	161.4(14)	161.3(7)	159.6(6)
C(10)-Ir(1)-P(1)	161.4(14)	161.2(7)	163.3(6)
C(5)-Ir(1)-C(6)	39.6(2)	39.2(9)	39.8(9)
C(10)-Ir(1)-C(9)	37.2(3)	37.1(9)	37.0(8)
C(5)-Ir(1)-C(9)	81.0(13)	96.7(9)	97.2(9)
C(6)-Ir(1)-C(10)	81.0(13)	88.9(9)	89.7(8)
C(5)-Ir(1)-C(10)	93.5(14)	81.3(9)	80.4(9)
C(6)-Ir(1)-C(9)	93.5(14)	80.0(9)	81.8(8)

and $H1_{syn}$ appear at δ 0.44–1.42 and 1.28–1.66, see Table 1. The relative upfield chemical shift position for H3 clearly reflect the *exo-syn* configuration of the 1-3-η pentadienyl ligand in these complexes. This proposal was also confirmed by ^1H-^1H ROESY experiment, which show strong interactions between the spatial orientation of H2 and H4 in compound **7**. In the $^{13}C\{^1H\}$ NMR spectra, C4 and C5′ appear at high frequency as expected for a terminal double bond non-coordinated, while C1, C2 and C3 are characteristic of an η^3-allylic coordination, see Table 2. The $^{31}P\{^1H\}$ spectra of **7**, **8** and **9b** showed singlets at δ 10.2, 5.3 and −52.7, respectively. The $^{13}C\{^1H\}$ NMR spectrum of **9a** exhibits all pattern of resonances as doublets due to phosphorus coupling. The chemical shifts are characteristic of the 1,4-5′-η-pentadienyl bonding mode: The uncomplexed carbon atoms C2 and C3 resonate at higher frequency [δ 136.8 (d, 12.5 Hz) and 138.3 (d, 4.7 Hz)], while the iridium coordinated atoms C1, C4 and C5′ at upfield, at 17.9 (d, 9.3 Hz), 56.1 (d, 15.6) and 25.9 (d, 6.2), respectively. In the $^{31}P\{^1H\}$ NMR spectrum the signal of the phosphorus atom resonates at −53.7 ppm.

According to ^1H NMR compound **9a** is the dominant species in the equilibrium mixture with **9b**, the ratio observed was 2:1. Several reactions with different amounts of lithium pentadienide (3–8 equiv) were carried out to check if the equilibrium of the mixture between **9a** and **9b** could change. In each case, the same ratio was observed. Also, an experiment in an NMR tube with the mixture of isomers in C_6D_6, was heated in an oil bath at 65 °C for 12 h, the spectra were obtained at 65 °C, and also after cooling the sample at room temperature, giving the same ratio of 2:1 for **9a** and **9b**, respectively. In contrast, in the chemistry of **7** and **8**, with the triphenyl- and tris(*iso*-propyl) phosphine ligands, the 1,4-5′-η-pentadienyl bonding mode is not detected by NMR. As already mentioned, this different behavior is explained in terms of less steric interactions of the trimethylphosphine in compounds **9a** and **9b**. The chemistry of electron rich pentadienyl iridium phosphine complexes obtained from $IrCl(PR_3)_3$ (R = Me, Et), (Scheme 1), as well as the Vaska's complex $Ir(Cl(CO)(PPh_3)_2$ (Scheme 2), in presence of potassium pentadienide, affords similar bonding modes. The crystalline structures of **7**, **8** and **9b** will be discussed along with **10** and **11a**, *vide infra*.

2.2.2. 2,4-dimethyl-pentadienyl complexes

The favorability of the η^5-*U* pentadienyl coordination, instead of η^3 or η^1, by the incorporation of methyl substituents in the pentadienyl ligands is well known [14]. In order to study the effects of the double methyl substitution in C2 and C4, compounds [(η^4-COD)Ir(1-3-η-$CH_2CMeCHCMeCH_2$)PPh_3] (**10**) and the mixture of isomers [(η^4-COD)Ir(1,4-5′-η-$CH_2CMeCHCMeCH_2$)PMe_3] (**11a**) and [(η^4-COD)Ir(1-3-η-$CH_2CMeCHCMeCH_2$)PMe_3] (**11b**) were isolated by addition of one equiv of PPh_3 and PMe_3 to compound **2** in THF at

Table 6
Selected bond lengths (Å) and angles (°) of pentadienyl compounds **2**, **7**, **8**, **9b**, **10** and **11a**.

Bond lengths (Å)						
	2	7	8	9b	10	11a
Ir1-C1	2.141(8)	2.126(7)	2.145(4)	2.143(3)	2.117(8)	2.128(6)
Ir1-C2	2.240(5)	2.132(7)	2.132(4)	2.120(4)	2.150(9)	
Ir1-C3	2.284(5)	2.329(8)	2.360(4)	2.291(3)	2.337(7)	
Ir1-C5	2.112(5)	2.129(8)	2.160(4)	2.141(3)	2.148(7)	2.136(6)
Ir1-C6	2.092(6)	2.134(7)	2.120(4)	2.136(3)	2.134(7)	2.131(7)
Ir1-C9	2.167(5)	2.172(7)	2.167(4)	2.169(3)	2.182(7)	2.235(6)
Ir1-C10	2.158(8)	2.216(6)	2.192(4)	2.188(3)	2.213(8)	2.236(6)
Ir1-P1		2.342(2)	2.4048(10)	2.3386(8)	2.348(2)	2.3511(16)
C1-C2	1.430(9)	1.431(11)	1.416(6)	1.422(6)	1.461(10)	1.491(9)
C2-C3	1.401(8)	1.396(11)	1.414(6)	1.423(6)	1.424(11)	1.317(10)
C3-C4		1.444(11)	1.470(7)	1.448(6)	1.469(10)	
C4-C4A		1.309(12)	1.261(7)	1.318(6)	1.334(11)	
C5-C6	1.442(9)	1.431(10)	1.437(6)	1.432(5)	1.449(12)	1.434(9)
C9-C10	1.401(8)	1.422(10)	1.412(6)	1.400(5)	1.416(10)	1.398(9)
Ir1-C1A	2.266(6)					2.157(6)
Ir1-C2A	2.235(6)					2.210(6)
C1A-C2A						1.422(9)
C2A-C3	1.442(8)					1.500(10)
Bond angles (°)						
	2	**7**	**8**	**9b**	**10**	**11a**
C1-C2-C3	119.1(6)	117.7(8)	117.3(4)	116.4(4)	111.7(7)	118.3(6)
C2-C3-C4		121.2(9)	119.1(5)	121.7(4)	127.7(8)	
C3-C4-C4A		127.6(10)	128.8(7)	126.2(5)	119.3(8)	
C1-Ir1-P1		96.3(3)	94.6(12)	94.3(12)	95.6(2)	83.0(19)
C3-Ir1-P1		93.5(2)	94.6(13)	89.8(11)	90.4(2)	
C5-Ir1-P1		101.7(2)	104.8(13)	100.0(9)	100.0(2)	96.1(19)
C6-Ir1-P1		140.8(2)	143.6(12)	138.8(11)	139.4(2)	139.4(2)
C9-Ir1-P1		116.8(2)	118.1(13)	118.5(10)	116.8(2)	119.2(17)
C10-Ir1-P1		87.7(2)	90.0(12)	87.7(9)	86.6(2)	84.7(18)
C1-Ir1-C10		175.1(3)	175.1(17)	177.9(14)	176.2(3)	161.1(2)
C1-Ir1-C9		140.5(3)	139.6(17)	141.2(14)	142.3(3)	157.7(3)
Ir1-C1-C2		70.6(4)	70.1(2)	69.7(2)	71.2(5)	73.0(4)
P1-Ir1-C6		140.8(2)	143.6(12)	138.8(11)	139.4(2)	133.7(18)
C5-Ir1-C3		158.5(3)	155.3(18)	163.1(14)	160.3(3)	
C5-Ir1-C1A						173.6(3)
C2-C3-C2A	126.9(5)					121.4(6)
C1A-C2A-C3	124.2(6)					117.8(6)
C1A-Ir1-P1						90.2(19)

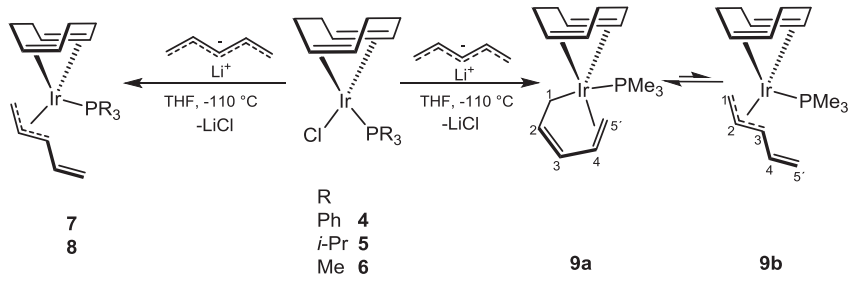

Scheme 4. Synthesis of **7**, **8** and isomers **9a** and **9b**.

room temperature, after stirring for 48 h and 5 min, in 53 and 26% yield, respectively, see Scheme 5.

Even after 1 h of stirring at room temperature, the mixture of **11a** and **11b**, in C_6D_6, shows the relative ratio of the products (2:1) remaining constant. According to the close similarity of the chemical behavior of the pentadienyl **9a** and **9b** (*vide supra*) and the corresponding 2,4-dimethyl-pentadienyl **11a** and **11b** (*vide infra*) it is evident that the influence of the methyl groups substituted in the pentadienyl ligand is not relevant as the far as the preference of different bonding modes is concerned.

These results contrast to those electron rich iridium pentadienyl complexes, obtained by Bleeke et al. [10–13], see Scheme 1, which clearly show the relevance of the electronic contribution of the methylated or unmethylated pentadienyl ligands on the final products. The products obtained by addition of PR_3 to **2**, Scheme 5, are more resembling to the equilibrium mixture found in the Vaska's type iridium pentadienyl complexes Ir(1-3-η-$CH_2CMeCHCMeCH_2$)(CO)$(PPh_3)_2$ and Ir(1,4-5′-η-$CH_2CMeCHCMeCH_2$)(CO)$(PPh_3)_2$, Scheme 2 [11]. This fact is attributed to the less electron donor complexes **11a** and **11b**, due to the presence of the COD ligand, which is acting as an acceptor ligand, and to the presence of only one donor phosphine.

The ^1H and $^{13}C\{^1H\}$ NMR spectra of compounds **10** and **11b** confirm the *exo-syn* configuration of the *W*-pentadienyl ligand, which exhibit upfield shifts of H3 at δ 1.90 and 2.25 (overlapped); C3 at δ 57.1 (d, 4.1) and 55.2 (d, 6.8), respectively.

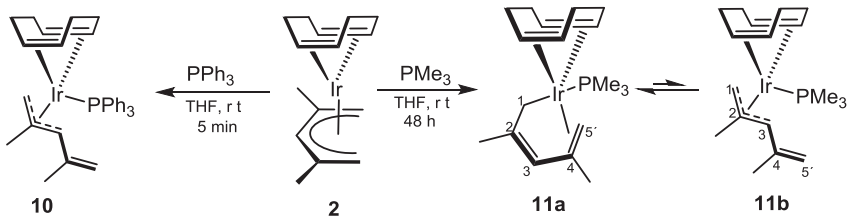

Scheme 5. Iridium phosphine compounds with the 2,4-dimethyl-pentadienyl ligand.

In the ^{1}H NMR spectrum of the equilibrium mixture of **11a** and **11b**, the major isomer **11a** shows the resonance of H3 at δ 5.91, which suggests an *anti* configuration of the *U*-pentadienyl ligand. In the ^{13}C{^{1}H} NMR spectrum of **11a**, non-coordinated carbon C2 and C3 resonates at δ 141.1 (d, 8.4) and 138.3 (d, 2.9), contrasting with those coordinated to iridium in **11 b** at δ 71.1 (d, 6.3) and 55.2 (d, 6.8).

With the objective of establishing factors that favor the stabilization of the equilibrium mixture observed for **11a** and **11b**, subsequent NMR experiments were carried out; such as adding PMe_3 to a $CDCl_3$ solution of **2** in an air-sensitive NMR tube, under N_2 atmosphere at −90 °C. There was evidence of the exclusive formation of **11a**, but once the reaction reached room temperature the presence of **11b** was corroborated. After 2 h the equilibrium mixture of **11a** and **11b** was detected in a 1:1 ratio. According to these results, reaction of **2** with 1.2 equiv of PMe_3 was monitored at different temperatures in the interest to determine if isomer **11b** could be obtained as the preferential product. The experiment, through the ^{31}P NMR, was carried out in CD_2Cl_2 from −90 °C until 30 °C, and in C_7D_8 from 25 °C until 100 °C. In Fig. 2 monitoring of reaction is shown from −60 °C until 100 °C, and then, the mixture in solution was going back to room temperature.

The reaction mixture at −60 °C showed free PMe_3, a minimum amount of **11a**, **11b** and a major new species assigned as (η^4-COD)Ir[1-3-η-CH_2C(Me)CHC(Me)CH_2](PMe_3) (**11c**) at δ −59.1. This intermediate species **11c** is proposed based on similar iridium η^5-pentadienyl complexes, that has shown the interconversion from the *U*-conformation into the corresponding 1-3-η-*W*-pentadienyl isomers [12], (*vide infra*).

At − 40 °C the PMe_3 has been already consumed, **11c** is the major species in solution, along with a minimum amount of **11a** and traces of **11b**. At 0 °C, **11c** was totally consumed, **11a** was growing, and there were traces of **11b**. At room temperature **11a** and **11b** were present in 3.0:1.0 ratio, whereas at 100 °C the ratio changed to 1.0:~2.8. Finally, going back to room temperature the ratio of **11b** to **11a** was almost 1.0:1.0.

It should be mentioned that the experiment carried out in CD_2Cl_2 after reaching room temperature, and the same sample cooled once again at −80 and −40 °C, showed in all cases **11a** as the major compound. In view of the above, a tentative mechanism is proposed as described in Scheme 6. Firstly, the addition of PMe_3 to **2** affords initially **11c**, which acts as an intermediary species to give **11a,** and in turn **11a** rearranges to **11b**. Once **11b** is formed it can interconvert to **11a**, however, **11a** cannot interconvert into **11c**. The interconversion of **11c** into **11b** involved coordination of the terminal double bond to give the bonding mode 1,4-5′-η observed for **11a**, and it is proposed that the isomerization of **11a** into **11b** occurred through coordinatively unsaturated intermediates such as (η^4-COD)Ir[η^1-$CH_2CHCHCHCH_2$](PMe_3) (**i**) and the rotation of the C3-C4 bond to afford (ii) which induced the transformation to **11b**.

The similarity of the ^{13}C{^{1}H} NMR spectrum of **11c**, at −40 °C in CD_2Cl_2, with the analogue of Ir[1-3-η-CH_2C(Me)CHC(Me)

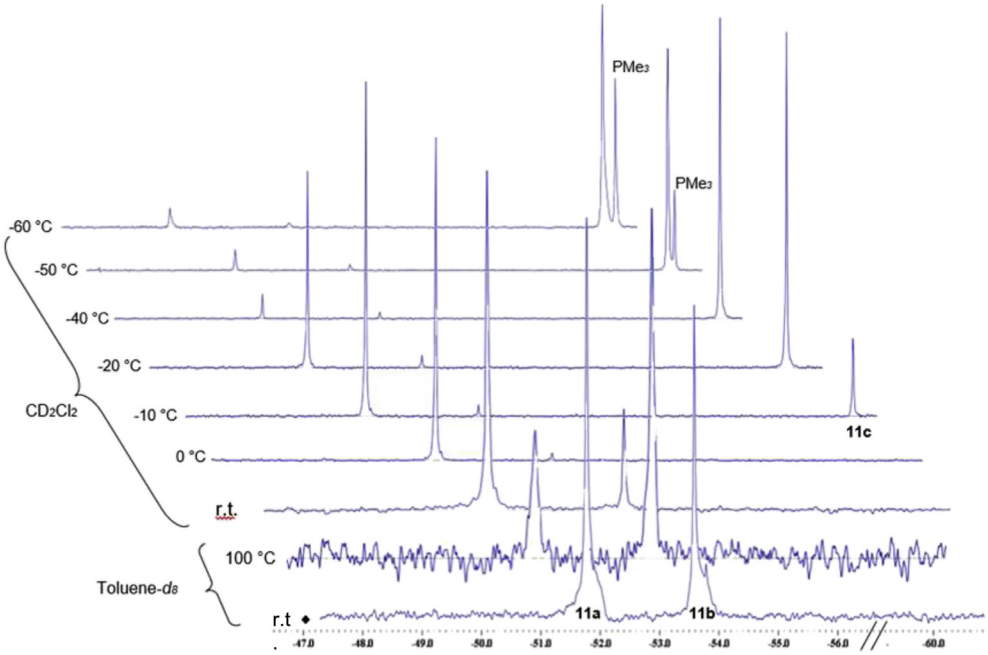

Fig. 2. ^{31}P{^{1}H} NMR (VT in CD_2Cl_2 and C_7D_8) of the reaction between **2** and PMe_3.

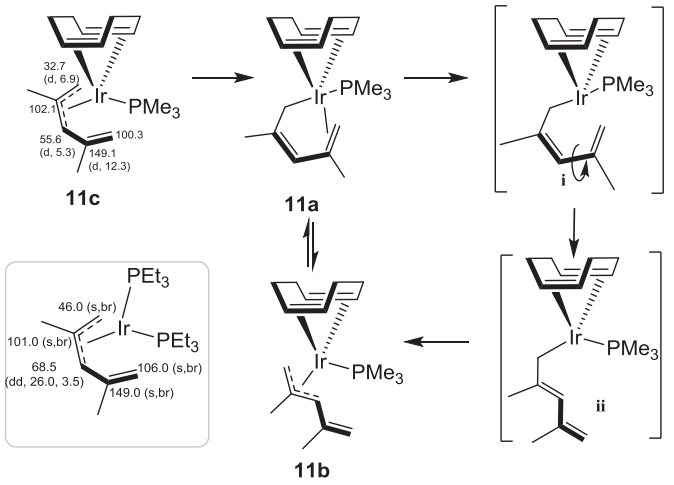

Scheme 6. Proposed mechanism of the formation of the equilibrium mixture of **11a** and **11b**.

$CH_2](PEt_3)_2$ [12], at −80 °C in C_7D_8, as described in Scheme 6, supports the same bonding mode with an uncoordinated terminal double bond at δ ~149.1 and ~100.3 for C3 and C4, respectively.

The existence of the equilibrium mixture of two different bonding modes (σ-allyl-π-olefin and σ,π-allyl) in **11a** and **11b**, as well as **9a** and **9b**, is attributed to two complementary factors: the more sterically demanding bonding mode 1,4-5′-η *vs.* 1-3-η and the small cone angle of the tertiary phosphine.

In order to understand in more detail the role of the phosphine ligands, we decide to synthesize the monosubstituted complex [(η^4-COD)IrCl(PMe_2Ph)] with a higher cone angle (PMe_2Ph, 122°) than PMe_3, following the synthetic procedure described for compound **6**. However, a mixture of the mono- and disubstituted complexes [(η^4-COD)IrCl($PMe_2Ph)_n$] (n = 1, 2) was obtained, efforts to separate them were unsuccessful. A previous reported NMR study on the reaction of PMe_2Ph with the dimeric complex **1**, gives spectroscopic evidence of the easy exchange and loss of ligands, according to the species observed, and reported as [(η^4-COD)IrCl($PMe_2Ph)_n$] (n = 1, 2), [(η^4-COD)Ir($PMe_2Ph)_3$]$^+$, as well as [Ir$Cl(PMe_2Ph)_3$] and [Ir($PMe_2Ph)_5$]$^+$ [21]. Contrastingly, studies with the bulkier complex [(η^4-COD)IrCl(PPh_3)] [22] in presence of an excess of PPh_3 have shown a rapid self-exchange between free and coordinated PPh_3 instead of the formation of a five-coordinate bis-triphenylphosphine adduct (η^4-COD)IrCl($PPh_3)_2$ [4b].

The pentadienyl ligand of compound **7** reacts in presence of chloroform, showing to be quite labile and favoring the regeneration of **4**. Compound **7** showed after 24 h in $CDCl_3$ the regeneration of compound **4** in 1:1 ratio; besides the crude product from the metathesis reaction of **7**, in presence of LiCl, displayed the formation of **4** in non-chlorinated solvents. Similarly, in the synthesis of the allylic compound (η^4-COD)Ir(2-Me-η^3-C_3H_4) [8], the formation of side products (η^4-COD)IrX(PH(*t*-Bu)$_2$) (X = Cl, Br) have already been obtained, as a result of the presence of residues of LiX in the mixture of reaction. The lability of the pentadienyl ligand in bulkier compounds **8** and **10** hampered the detection of the molecular ion in the mass spectra. Both compounds showed, through the ESI + TOF-MS technique, using acetonitrile, a peak detected at 502.2197 and 604.1737 *m/z*, respectively, assigned to [(η^4-COD)Ir(PR_3)(MeCN)]$^+$ (R = *i*-Pr, Ph). Similar peak as the one detected for **8** was observed for compound **5** at 502.2215 *m/z*. Compounds [(η^4-COD)Ir(PPh_3)(MeCN)]BF_4 [23] and [(η^4-COD)Ir(PMe_3)(MeCN)]BF_4 [4a] have already been isolated and previously reported.

Further characterization of **7**, as well as the mixtures of **9a**, **9b** and **11a** and **11b** was accomplished also by ESI + TOF-MS giving the corresponding molecular ion.

As observed from the NMR analysis, the same chemical structures are observed in solid-state and in solution for **2**, **7**, **8**, **9b**, **10** and **11a**, *vide infra*.

2.2.3. Crystal structures

The single crystal X-ray structural determination of compounds **4**–**6** was carried out, allowing **5** and **6** to complete the crystallographic study of the precursors used in this work. Compound **4** has already been reported [24], and its molecular structure is included in the Supplementary Data. The ORTEP plots of **5** and **6** are shown in Figs. 3 and 4, respectively. The summary of experimental data is listed in Table 3, including compound **4** for comparison purposes,

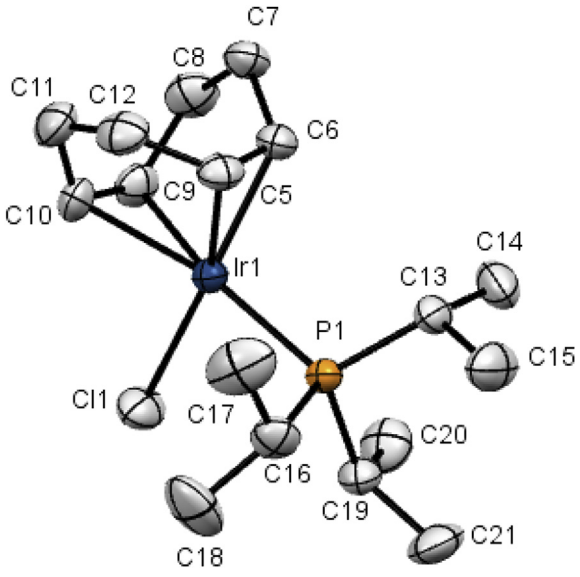

Fig. 3. Molecular structure of compound (η^4-COD)Ir(Cl)(P(*i*-Pr_3) (**5**). Hydrogen atoms have been omitted for the sake of clarity.

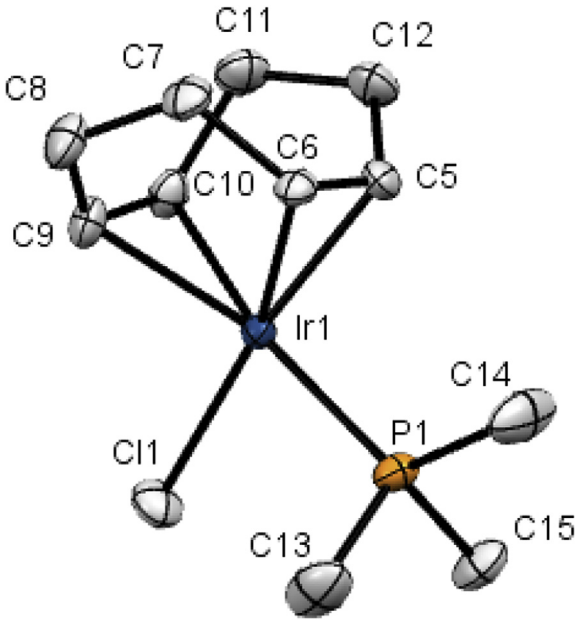

Fig. 4. Molecular structure of compound (η^4-COD)Ir(Cl)(PMe_3) (**6**). Hydrogen atoms have been omitted for the sake of clarity.

and selected bond lengths (Å) and angles (°) are described in Table 5. The overall structures of **4**–**6** can be described as approximately square-planar, with the COD ligand occupying two coordination sites, and the chlorine atom and phosphine ligand at the other two sites.

The bond angles about the iridium center show carbon atoms C10 and C5 opposite to the phosphorus and chlorine atoms, respectively, the latter being in a *cis* arrangement (~87–90°). The higher cone angle of the coordinated phosphine to the iridium atom, shows the longest bond length: [$P(iPr)_3$, 2.3522(5) > PPh_3, 2.3172(9) > PMe_3, 2.2993(5) Å].

The elongation of the double bonds C5-C6 are longer [range: 1.428(3)-1.433(3) Å] than those for C9-C10 [range: 1.389(11)-1.396(3) Å], while the Ir-C5, Ir-C6 [range: 2.101(2)-2.141(2) Å] show shorter bonds compared to those of Ir-C9, Ir-C10 [range: 2.180(3)-2.214(2) Å]. The asymmetry of the coordination of the COD ligand is also observed for the corresponding (η^4-COD)Ir(pentadienyl)(PR_3) derivatives, *vide infra*.

The solid state structures of **7**, **8**, **9b**, **10** and **11a** are presented in Figs. 5–9. The crystal data and selected bond lengths and angles are provided in Tables 4 and 6, respectively. The crystal structure determination of compound **10** revealed the presence of two independent molecules in the unit cell. These molecules are structurally identical, and for clarity, the crystal data and structure of only one is described here.

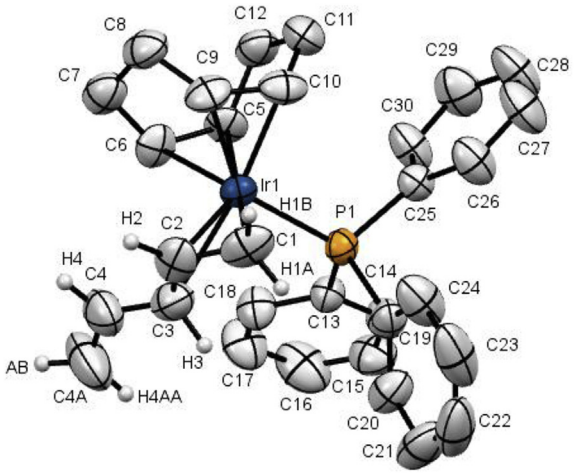

Fig. 5. Molecular structure of (η^4-COD)Ir(1-3-η-$CH_2CHCHCHCH_2$)(PPh_3) (**7**). Hydrogen atoms have been omitted for the sake of clarity, except those of the pentadienyl ligand.

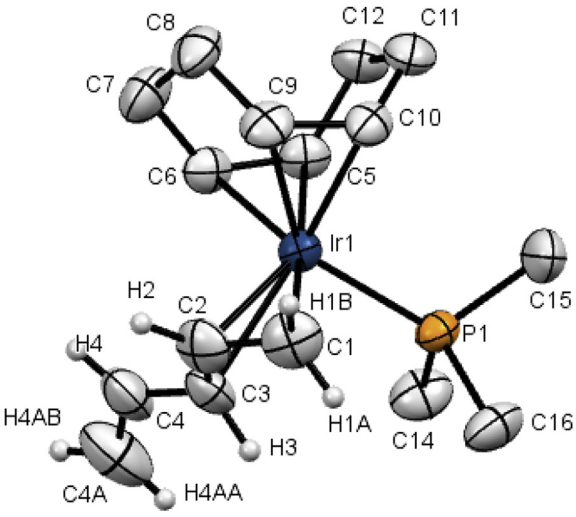

Fig. 6. Molecular structure of (η^4-COD)Ir(1-3-η-$CH_2CHCHCHCH_2$)(P(*i*-Pr)$_3$) (**8**). Hydrogen atoms have been omitted for the sake of clarity, except those of the pentadienyl ligand.

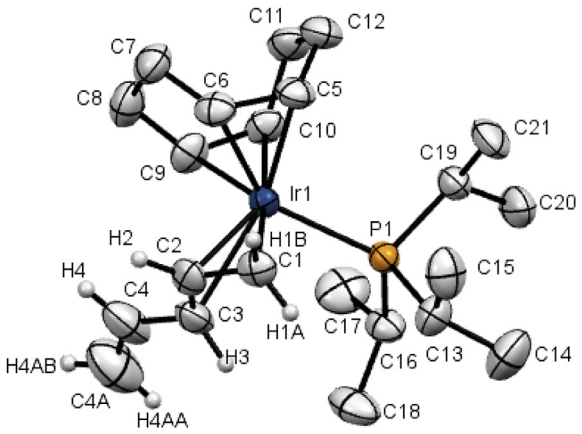

Fig. 7. Molecular structure of (η^4-COD)Ir(1-3-η-$CH_2CHCHCHCH_2$)(PMe_3) (**9b**). Hydrogen atoms have been omitted for the sake of clarity, except those of the pentadienyl ligand.

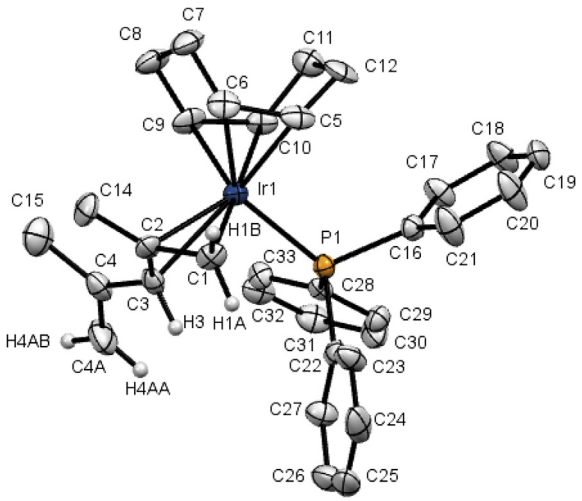

Fig. 8. Molecular structure of (η^4-COD)Ir(1-3-η-$CH_2CMeCHCMeCH_2$)(PPh_3) (**10**). Hydrogen atoms have been omitted for the sake of clarity, except those of the pentadienyl ligand.

In general, the structural parameters for complexes **7**, **8**, **9b** and **10** correspond fairly close to each other. All five-coordinate complexes **7**, **8**, **9b**, **10** adopt a geometric distortion from square-pyramidal (SP) rather more than a trigonal-bipyramidal (TBPY), while **11a** shows an intermediacy between the geometric extremes of SP and TBPY structures, such as that observed for (η^4-COD)$_2$IrCl [16].

This is supported according to the τ parameter [16,25,26], calculated using the mid-points of both C5=C6 and C9=C10 double bonds of the COD ligands with the corresponding C1 and C3 of the allylic fragment, giving for **7** (τ = 0.295), **8** (τ = 0.346), **9b** (τ = 0.216), **10** (τ = 0.265), while the mid-points of C5=C6 and C9=C10 double bonds of the COD ligands with C1 and the mid-point of C1A=C2A of the pentadienyl ligand for **11A** gives a higher value (τ = 0.584), which suggests similar geometry than (η^4-COD)$_2$IrCl (τ = 0.52) [16], and [(η^4-COD)Ir(1-2,5-η-$CH_2CHCHCHSO_2$)(PR_3)] (R = Me, τ = 0.550;

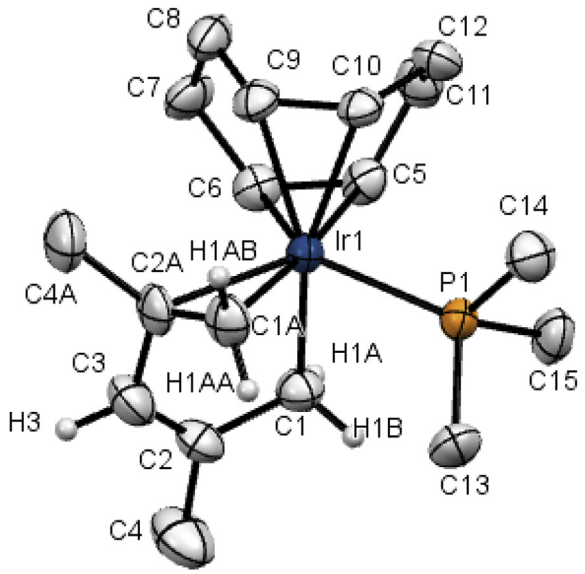

Fig. 9. Molecular structure of (η^4-COD)Ir(1,4-5′-η-CH_2CMeCHCMeCH_2)(PPh_3) (**11a**). Hydrogen atoms have been omitted for the sake of clarity, except those of the pentadienyl ligand.

Ph, τ = 0.0.617) [5]. All these structures contrast to the SP geometry found in [(η^4-COD)Ir(η^3-CH_2CMeCH_2)(PH(*t*-Bu)$_2$)] (τ = 0.0006) [8], [(η^4-COD)Ir(η^3-CH_2CHCH_2)(P(OMe)$_3$)] (τ = 0.045) [9] and [Ir(η^4-COD)(PMe_3)$_3$]$^+$ (τ = 0.058) [27].

The elongation of the double bonds C5-C6 and C9-C10 are asymmetric, where the C5-C6 double bonds are larger [range: 1.431(10)-1.449(12) Å] than C9-C10 [range: 1.398(9)-1.422(10) Å]. Similarly, the bond lengths between iridium and the double carbon bonds also show asymmetry with shorter distances for Ir-C5 and Ir-C6 [range: 2.120(4)-2.160(4) Å], and longer distances for Ir-C9 and Ir-C10 [range: 2.167(4)-2.236(6) Å]. Related asymmetry was observed for (η^4-COD)$_2$IrCl [16] and with distorted TBPY geometries for Ir(η^4-COD)(1-2,5-η-CH_2CHCHCHSO_2)(L) (L = PMe_3, PPh_3) [5].

The bonding parameters within the pentadienyl ligands are quite similar, where the enyl fragment in all complexes is coordinated to the iridium center, which is clearly demonstrated by the enlargement of the bond lengths C1-C2-C3 [1.416–1.461(10) and 1.396–1.424(11) Å] due to the backbonding of the π-ligand. In contrast, the terminal double bonds, which are not coordinated, show the typical sp^2 C4-C4A bond lengths between 1.261(7) and 1.334(11) Å. The C1-C2-C3-C4 and C2-C3-C4-C4A torsional angles for the η^3-pentadienyl complexes **7**, **8** and **9b** [average: −174.8, −164.0°] and **10** [176.7(8), −158.5(9)°] imply that the ligand can be described as a W conformers with a *exo-syn* geometry. In contrast, compound **11a** displays a *pseudo*-six-membered iridacyle structure with the metal coordination η^1 to C1, and η^2 to C1A and C2A. The torsional angles of **11a** [C(1)-C(2)-C(3)-C(2A), −3.9(11)° and C(2)-C(3)-C(2A)-C(1A), −66.0(10)°] give evidence of the pentadienyl ligand being U shaped, and where bond lengths of alternating double and single bonds of the *pseudo*-iridium ring are C1-C2, 1.491(9), C2-C3, 1.317(10), C3-C2A, 1.500(10) and C2A-C1A, 1.422(9) Å.

The Ir-P bond lengths exhibited the longest value for the bulky tris-*iso*-propylphosphine complex **8** [2.4048(10) Å], followed by the triphenylphosphine complexes **7** [2.342(2) Å], **10** [2.348(2) Å], and the trimethylphosphine **9b** [2.3386(8) Å], being a particularly long bond length observed for **11a** (2.3511(16) Å).

The molecular structures of electron-rich complexes Ir(PEt_3)$_3$(1,4-5′-η-CH_2CHCHCHCH_2) and Ir(PMe_3)$_3$(1,4-5′-η-CH_2CMeCHCMeCH_2), as well as Ir(CO)(PPh_3)$_2$(1,4-5′-η-CH_2CMeCHCMeCH_2) differs from **11a**. Those have been described as a distorted octahedron, in which the six coordinated sites are occupied by C1, C4 and C5 of the pentadienyl ligand and the three PR_3 (R = Et, Me) or two PPh_3 and CO. The octahedral geometry in both electron-rich complexes and Vaska's derivative is justified by the substantial back-bonding as evidenced by the relative long C4-C5 bond lengths [1.454(17), 1.465(12) and 1.430 (11) Å] and the Ir-C4-C5 bond angles [69.0(7), 68.9(5), 68.1(4)°], respectively. Based on that, these molecular structures of Ir(PEt_3)$_3$(1,4-5′-η-CH_2CHCHCHCH_2), Ir(PMe_3)$_3$(1,4-5′-η-CH_2CMeCHCMeCH_2) and Ir(CO)(PPh_3)$_2$(1,4-5′-η-CH_2CMeCHCMeCH_2) have been proposed as an approximation to a metallacyclopropane in which the iridium center is formally oxidized to Ir(III) [11]. In compound **11a** there is a shorter bond length of 1.422(9) Å and a wider bond angle 73.0(4)° which supports the preference of Ir(I) for a less electron rich complex **11a**.

3. Concluding remarks

The products **7**–**11** obtained by reaction of **1** with phosphines depend on the nature of the phosphorus donor ligand, the steric effect being predominant in the preference of the pentadienyl bonding mode. The 1-3-η-pentadienyl complexes **7**, **8** and **10** are formed in presence of the bulkier phosphines P(*i*-Pr)$_3$ and PPh_3, while the less bulky PMe_3 favor an equilibrium between the 1,4-5′-η-pentadienyl and 1-3-η-pentadienyl complexes **9a**, **9b** and **11a**, **11b** in a ratio of 2:1, respectively. The ^{31}P NMR of the reaction of **2** and PMe_3, in different solvents and temperatures, gave spectroscopic evidence of the interconversion bonding modes of the pentadienyl ligand, where the *pseudo*-metallacycle (η^4-COD)Ir(2,4-dimethyl-1,4-5′-η-pentadiene)(PMe_3) (**11a**) correspond to the kinetic product, and (η^4-COD)Ir(2,4-dimethyl-1-3-η-pentadienyl)(PMe_3) (**11b**) as the thermodynamic one. There was also the detection of the pentadienyl ligand in a U conformer **11c**, being the first species formed in the addition reaction of PMe_3 into compound **2**, without spectroscopic evidence of the intermediacy of η^1 bonding mode species.

The π-accepting COD ligand play the role of an ancillary and spectator ligand in these iridium complexes, showing a robust iridium-diene bonding. The high degree of π back-bonding of the pentadienyl and cyclooctadiene ligands in complexes **9**, **10** and **11** contrast strongly with the reactivity of the pentadienyl ligands coordinated to electron rich Ir(PR_3)$_3$ (R = Et, Me) moieties, where a C-H activation of the pentadienyl ligand favors the formation of 1,5-η bonding mode in the iridacyclohexadiene complex. As observed for all compounds in Scheme 1, the influence of the inductive effect by the presence or absence of methyl substituents on the pentadienyl ligands, along with the steric bulkiness of the coordinated phosphines, leads to the following outcomes: (a) the exclusive generation of metallacycles; (b) an equilibrium mixture of metallacycle Ir(III) and *pseudo*-metallacycles Ir(I) and (c) the exclusive formation of the *pseudo*-metallacycles Ir(I) complexes. In the cyclooctadiene phosphine chemistry described in this paper, the presence or absence of methyl substituents in the pentadienyl ligands does not modify the preference of the bonding modes in the (η^4-COD)Ir(PR_3) (R = *i*-Pr, Ph) moieties, which suggests that the methyl substituents in a W-shaped, such as 2,4-dimethyl-η^3-syn-pentadienyl ligand in **11b** does not experience significant steric contact, as proposed for Ir(2,4-dimethyl-1-3-η-pentadienyl)(CO)(PPh_3)$_2$ [11]. The reaction of IrCl(CO)(PPh_3)$_2$ with potassium 2,4-dimethyl-pentadienide produced an analogue equilibrium mixture, with similar bonding modes 1,4-5′-η and 1-3-η-pentadienyl, as observed for **11a**, **11b**, Schemes 2 and 5, respectively. Considering the electronic and steric properties of the different Ir(η^4-COD)(PMe_3) and Ir(CO)(PPh_3)$_2$ moieties which are coordinated to pentadienyl complexes, is interesting to observe

that the chemical structures of Ir(η^4-COD)(1,4-5′-η-$CH_2CHMeCHCMeCH_2$)(PMe_3) (**11a**) and Ir(1,4-5′-η-$CH_2CHMeCHCMeCH_2$)(CO)(PPh_3)$_2$ [11] show quite similar bond lengths in their corresponding pentadienyl ligands [Ir-C1, 2.128(6), 2.143(7); Ir-C4, 2.210(6), 2.214(8); Ir-C5′, 2.157(6), 2.141(7); C1-C2, 1.491(9), 1.506(10); C2-C3, 1.317(10), 1.309(13); C3-C4, 1.500(10), 1.484(12); C4-C5′, 1.422(9), 1.430(11) Å, respectively]. The latter suggests a counterbalance between the electronic and steric contribution of the corresponding ligands: on one side [(η^4-COD), PMe_3], on another [CO, (PPh_3)$_2$].

In general terms, and in agreement with the influence of electronic and steric effects on the preferential bonding modes of iridium pentadienyl complexes, it could be concluded that the 1-3-η-pentadienyl complexes are favored in presence of π-ligands and bulkier phosphines, such as PPh_3 and P(*i*-Pr)$_3$, while they are definitively not favored in presence of electron rich precursors $IrCl(PR_3)_3$. The 1,5-η-iridacyclohexadiene complexes are fully dependent on the electronic effects, and finally the 1,4-5′-η-pentadienyl complexes play an intermediate role, depending on the modulation of those electronic and steric effects.

4. Experimental section

4.1. General procedures

Standard inert-atmosphere experimental techniques were used for all syntheses and sample manipulations. Solvents were dried by standard methods (hexane and pentane with CaH_2, diethyl ether and THF with Na/benzophenone, CH_2Cl_2 and $CHCl_3$ with $CaCl_2$, benzene with Na) and distilled under nitrogen prior to use. Compounds $CH_2CRCHCRCH_2SnMe_3$, (R = H [28a,b], Me [28c]), [(η^4-COD)Ir(μ-Cl)]$_2$ (**1**) [2d], (η^4-COD)Ir(Cl)(PPh_3) (**4**) [2a,2e,5], were prepared according to literature procedures. All other chemicals were used as purchased from Sigma-Aldrich, Strem Chemicals, Merck, Pressure Chemicals, Cambridge Isotopes and J. T. Baker. All compresses gases were obtained from Infra: argon and nitrogen and were used as supplied without purification. Melting points were uncorrected. Elemental analyses were performed with a Thermo-Finnigan Flash 1112 combustion analyzer, at the Chemistry Department at Cinvestav. Infrared spectra were recorded on FT-IR Perkin-Elmer16F and 1600 spectrometers using KBr pellets, chloroform, or benzene solutions. The ^{1}H, ^{13}C, and ^{31}P NMR spectra were recorded on Jeol GSX-270, Eclipse 400 MHz, Eclipse 500 MHz or Bruker 300 MHz spectrometers in deoxygenated, deuterated solvents. NMR chemical shifts are reported relative to their residual protium resonances in the solvent, and ^{31}P NMR chemical shifts relative to 85% H_3PO_4. Mass spectra were recorded on a Hewlett-Packard HP-5990A spectrometer, while high resolution mass spectra were obtained by Agilent LC/MSD TOF (ESI) spectrometer with APCI as the ionization source. Melting points were determined in a Melt-Temp Gallenkamp (digital) instrument and have not been corrected.

The crystal structure determination was carried out in diffractometers Bruker Nonius, Kappa CCD or Bruker Instrument Service vV6.2.6. The resolution and refinement were done by SHELXS-97 [29] and SHELXL-97 [29] included in the software WingX, also cell refinement and data reduction: SAINT V8.38A (Bruker AXS Inc.,2017). Program(s) to solve structure XT, VERSION 2014/5, refined structure SHEXL2014/7 [29], and molecular graphics, XP V 5.1 (Bruker, 1998) and software used to prepare material for publication: CIFTAB V 2013/2 [29]. A summary of crystal data collection and refinement parameters of compounds is given in Tables 3 and 4. The ellipsoids were drawn at 50% probability for all crystalline structures.

4.2. Synthesis of (η^4-COD)Ir(η^5-$CH_2CMeCHCMeCH_2$) (**2**)

A THF solution (30 mL) of [Ir(η^4-COD)(μ-Cl)$_2$]$_2$ (509 mg, 0.76 mmol) was filtered, and $Me_3SnCH_2CMeCHCMeCH_2$ (779.0 mg, 3.03 mmol) previously dissolved in THF (1 mL) was added. The orange-red reaction mixture immediately changed to bright yellow, and was stirred for 1 h. The solution was cooled (−110 °C) and the solvent was removed under vacuum until ~ 8.0 mL [30]. Distilled water (~2.0 mL) was added, and the solution stirred for 5 min. Extractions with diethyl ether, filtration and the solvent removed under vacuum afforded a pale-yellow oily product, which was put in the freezer (−72 °C) for 12 h. A solid was obtained and kept under vacuum at −78 °C (acetone/dry ice). The solid was kept, under nitrogen, in the freezer at −72 °C. The yield of **2** is 90% (682.0 mg, 0.68 mmol). M. p. 60–62 °C. IR ($CHCl_3$, cm^{-1}): 2959 (s), 2929 (s), 2873 (s), 1461 (m,br), 1373 (w,br), 1001 (w), 892 (w). LREI: *m*/*z* 396.1430. Anal. Calcd for $C_{15}H_{23}Ir$: C, 45.55; H, 5.86. Found: C, 45.56; H, 6.51.

4.3. Synthesis of (η^4-COD)Ir(η^5-$CH_2CHCHCHCH_2$) (**3**)

Method (*a*). Under nitrogen atmosphere, *n*-BuLi (0.23 mL, 0.33 mmol, 1.6 M) and 1,4-pentadiene (34.0 μL, 0.33 mmol) were added to a cold (−110 °C) THF solution (1.0 mL). The yellow solution was stirred 15 min. After this time the solution was changed to an ice-bath turning to a strong-orange color and stirred 10 min. The lithium pentadienide was added to a cold (−110 °C) THF (15 mL) solution of [Ir(η^4-COD)(μ-Cl)$_2$]$_2$ (100.0 mg, 0.15 mmol). The solution turned pale yellow and it was stirred 15 min. The solution was evaporated at low temperature (−110 °C) [30] affording an amber-yellow oil, which was analyzed through the ^{1}H NMR.

Method (*b*). Following a similar synthetic procedure as described for compound **2**, a diethyl ether solution (4 mL) of [(η^4-COD) Ir(μ-Cl)$_2$]$_2$ (173.0 mg, 0.26 mmol) and *n*-$Bu_3SnCH_2CHCHCHCH_2$ (368.0 mg, 1.04 mmol) previously dissolved in THF (1 mL) was added. The bright orange reaction mixture immediately changes to yellow, and it was stirred for 15 min. Distilled water (~3.0 mL) was added, and the solution stirred for 5 min and the ethereal phase was filtered. The solvent was removed in vacuo at low temperature affording an amber-yellow oily product in very low yield. Attempts to solidify **3** were unsuccessful, and only the spectroscopic characterization was carried out through the IR and ^{1}H and ^{13}C{^{1}H} NMR. IR ($CHCl_3$, cm^{-1}): 2938 (vs), 2873 (vs), 2728 (vw), 1712 (w,br), 1461 (s), 1379 (m), 1137 (vw), 1290 (vw), 1222 (vw), 1136 (w,br), 1063 (w,br), 1013 (vw,br), 982 (w,br), 898 (w,br), 867 (w,br), 752 (w,br).

4.4. Synthesis of (η^4-COD)Ir(Cl)(P(*i*-Pr)$_3$) (**5**)

A cold solution (−100 °C, N_2 liquid/EtOH) of dimer **1** (400.0 mg, 0.60 mmol) in THF (40 mL) tris-*iso*-propylphosphine (0.23 mL, 1.19 mmol) was added or dropwise under argon atmosphere. Removing the cold bath, the resulting suspension was allowed to reach room temperature, filtered and the solvent concentrated to *c.a.* 8 mL and hexane (80 mL) added. A yellow solid precipitated was filtered and dry under vacuum, giving 95% yield (560.0 mg, 1.13 mmol). IR (KBr, cm^{-1}): 3017 (sh), 2965 (vs), 2931 (vs), 2873 (vs), 2834 (sh), 2730 (sh) 2578 (sh), 2343 (w, br), 1940 (w, br), 1740 (m, br), 1712 (m, br), 1633 (m, br), 1599 (m, br), 1548 (sh),.1459 (vs), 1386 (s), 1329 (s), 1329 (s), 1294 (m), 1244 (s), 1213 (sh), 1158 (m), 1090 (s), 1056 (s), 1030 (vs), 1001 (s), 928 (s), 969 (s), 928 (m), 881 (s), 814 (s), 696 (m), 648 (vs), 573 (m), 533 (s), 503 (s), 463 (m), 432 (m). ESI + TOF: *m*/*z* 502.2215; error: −0.552083 ppm, DBE 4.0 which correspond to [(COD)Ir(MeCN)(P(*i*-Pr)$_3$)]$^+$ [4a].

4.5. Synthesis of [(η^4-COD)Ir(Cl)(PMe_3)] (**6**)

The synthesis was carried out as described in the literature [5], but the THF concentrated to *c.a.* 8 mL and hexane (80 mL) added. A cream precipitate appeared which was filtered and dried under vacuum, affording the disubstituted compound (η^4-COD)Ir(Cl)(PMe_3)$_2$ [5,31] (17.0 mg, 0.035 mmol) in 2.9% yield. The remaining THF/hexane solution was evaporated under vacuum until dryness, to give an orange solid of **6** (410.0 mg, 1.04 mmol) in 88.0% yield and was stored in a refrigerator to avoid decomposition.

4.6. Synthesis of (η^4-COD)Ir(1-3-η-$CH_2CHCHCHCH_2$)(PPh_3) (**7**)

The reaction of the lithium pentadienide was carried out via a procedure similar to that described for **3** (method *a*), but with 1,4-pentadiene (34 μL, 0.33 mmol) and BuLi (0.13 mL, 0.33 mmol, 2.5 M). The lithium pentadienide prepared *in situ* was added to a cold (−110 °C) THF (15 mL) solution of (η^4-COD)Ir(Cl)(PPh_3) (150.0 mg, 0.25 mmol). The reaction mixture was stirred 5 min at −110 °C (EtOH/liq. N_2), changing immediately from strong-orange to pale-yellow. The solution was filtered and the solvent removed under vacuum. A minimum amount of pentane (~2 mL) was added to the oily residue affording, after evaporation of the solvent, a pale-yellow powder was dried in vacuo. Yield: 89% (140.0 mg, 0.22 mmol). M.p. 73-75 °C, dec. IR (C_6H_6, cm^{-1}): 3087 (s), 3070 (s), 3043 (s), 1955 (w), 1814 (m), 1620 (w), 1482 (vs), 1478 (vs), 1474 (vs), 1427 (w), 1091 (w,br), 1034 (s), 881 (w), 747 (w), 683 (vs), 667 (vs). ESI + TOF: *m/z* 631.2099; error: −0.2110 ppm, DBE 16. Anal. Calcd for $C_{31}H_{34}PIr$: C, 59.12; H, 5.44. Found: C, 59.17; H, 5.77.

4.7. Synthesis of (η^4-COD)Ir(1-3-η-$CH_2CHCHCHCH_2$)(*i*-PPr_3) (**8**)

The reaction of the lithium pentadienide was carried out via a similar procedure to that described for **3** (method *a*), but with 1,4-pentadiene (73 μL, 0.70 mmol) and BuLi (0.49 mL, 0.70 mmol, 1.6 M). The lithium pentadienide prepared *in situ* was added to a cold (−110 °C) THF (15 mL) solution of (η^4-COD)Ir(Cl)(P(*i*-Pr_3)) (174.3 mg, 0.15 mmol). The reaction mixture was stirred 5 min at −110 °C (EtOH/liq. N_2), changing immediately from strong-orange to strong-yellow. The solution was filtered and the solvent removed. A minimum amount of pentane (~2 mL) was added to the oily residue, which after treatment as described for **9a** and **9b** [32], afforded a yellow powder of **8** in 33% yield: (61.0 mg, 0.12 mmol). M.p. 92-94 °C, dec. IR (KBr, cm^{-1}): 3569 (w), 3401 (w, br), 3081 (vw), 3036 (w), 2958 (vs), 2913 (vs), 2861(vs), 2829 (vs), 2370 (vw, br), 1989 (vw, br), 1913 (vw, br), 1768 (vw), 1743 (vw), 1614 (s), 1497 (vw), 1466 (s), 1449 (s), 1399 (w), 1376 (m), 1359 (w), 1317 (m), 1284 (w), 1234 (m), 1200 (w), 1166 (w), 1150 (m), 1099 (vw), 1088 (vw), 1057 (w), 1027 (w), 993 (m), 957 (w), 923 (vw, br), 881 (s), 839 (w), 806 (vw), 786 (w), 674 (w), 643 (s), 629 (s), 593 (vw), 565 (w), 529 (s), 492 (m), 461 (m, br). ESI + TOF: Calcd. m/z 527.7425; Exp. m/z 502.219684, which correspond to $[(COD)Ir(MeCN)(P(i\text{-}Pr)_3)]^+$, ($C_{20}H_{38}PIr$, 501.69). Anal. Calcd for $C_{22}H_{40}PIr\cdot 2H_2O$: C, 47.66; H, 7.99. Found: C, 47.91; H, 7.39.

4.8. Synthesis of mixture of isomers (η^4-COD)Ir(1-3-η-$CH_2CHCHCHCH_2$)(PMe_3) (9a) and (η^4-COD)Ir[1,4-5′-η-$CH_2CHCHCHCH_2$](PMe_3) (**9b**)

The reaction of the lithium pentadienide was carried out via a similar procedure to that described for **3** (method *a*), but with 1,4-pentadiene (0.2 mL, 1.94 mmol) and BuLi (0.76 mL, 1.94 mmol, 2.5 M). The lithium pentadienide prepared *in situ* was added to a cold (−110 °C) THF (15 mL) solution of (η^4-COD)Ir(Cl)(PMe_3) (100.0 mg, 0.24 mmol). The solution turned colorless and reached room temperature under stirring for 12 h. The mixture was filtered and evaporated under vacuum affording an yellow oily-solid, which was turned into a powder using the following procedure [32]: the oily product, in the presence of a magnetic stirrer, and 0.5 mL of diethyl-ether was cooled under liquid nitrogen until the residue was frozen. The bottom surface of the Schlenk was rubbed with an external strong magnet, until the frozen residue turned to powder. Finally, the volatiles were removed in vacuo, and the sticky-solid was once again treated, as described above, with pentane (0.5 mL) and dried under vacuum. The mixture of isomers **9a** and **9b** was obtained as a beige solid in 60% yield (65.0 mg, 0.15 mmol). The pentane solution was kept at −4 °C, affording single crystals of **9b** which melts at 88−90 °C. IR ($CHCl_3$, cm^{-1}): 2958 (vs), 2931 (vs), 2728 (vw), 1712 (w,br), 1461 (s), 1379 (m), 1292 (vw), 1214 (m,br), 1136 (w,br), 1060 (w,br), 945 (w,br), 892 (w,br), 858 (w,br), 750 (w,br). ESI + TOF: *m/z* 445.1632; error: 0.2628 ppm, DBE 4. Anal. Calcd for $C_{16}H_{28}PIr\cdot H_2O$: C, 41.63; H, 6.55. Found: C, 42.05; H, 6.18.

4.9. Synthesis of (η^4-COD)Ir(1-3-η-$CH_2CMeCHCMeCH_2$)(PPh_3) (**10**)

Compound **2** (100 mg, 0.25 mmol) and PPh_3 (66.4 mg, 0.25 mmol) in THF (5 mL) were placed into a Schlenk flask equipped with a stir bar. The solution was stirred at room temperature for 48 h, filtered and evaporated under vacum. The yellow powder was dissolved in pentane and stored at −5 °C, to give yellow crystals in 53% yield (87 mg, 0.13 mmol). M. p. 133−135 °C. IR (KBr, cm^{-1}): 3048 (m), 3020 (vw), 2980 (s), 2964 (s), 2913 (s), 2857 (s), 2818 (s), 2661 (vw, br), 2627 (vw, br), 2566 (vw, br), 2364 (w), 2366 (w), 1964 (vw, br), 1936 (vw, br), 1910 (w, br), 1869 (vw, br), 1827(vw, br), 1617 (m), 1600 (m), 1583 (m), 1477 (m), 1432 (vs), 1376 (m), 1317 (m), 1236 (vw), 1214 (vw), 1194 (vw), 1178 (m), 1152 (m), 1116 (vw), 1085 (s), 1024 (s), 996 (s), 957 (vw), 906 (vw), 881 (m), 862 (m), 839 (m), 808 (vw), 783 (w), 736 (s), 697 (vs), 657 (sh), 615 (sh), 565 (sh), 529 (vs), 506 (s), 490 (s), 473,417 (m). ESI + TOF: Calcd. m/z 657.804; Exp. m/z 604.1737 which correspond to $[(COD)Ir(MeCN)(PPh_3)]^+$, ($C_{20}H_{38}PIr$, 603.7918). Anal. Calcd for $C_{33}H_{38}PIr$: C, 60.25; H, 5.82. Found: C, 60.41; H, 5.90.

4.10. Synthesis of mixture of isomers (η^4-COD)Ir(1-3-η-$CH_2CMeCHCMeCH_2$) (PMe_3) (11a) and (η^4-COD)Ir [1,4-5′-η-$CH_2CMeCHCMeCH_2$](PMe_3) (**11b**)

The reaction was carried out via a procedure similar to that described for **10**, but with PMe_3 (26.0 μL, 19.2 mg, 0.25 mmol). The addition of the PMe_3 showed an immediate change of color from pale-yellow to colorless. The solution was stirred for 5 min at room temperature. After filtration and evaporation under vacuum, an oily residue was obtained and crystallized with pentane at −5 °C to afford colorless crystals in 26% (31 mg, 0.07 mmol). M. p. 76−78 °C. IR (KBr, cm^{-1}): 3014 (m), 2975 (s), 2947 (s), 2908 (s), 2829 (vs), 2784 (w), 2706 (dw), 2633 (w), 2359 (w), 2263 (w), 2000 (w), 1857 (w), 1670 (m), 1483 (w), 1443 (s), 1424 (vs), 1359 (w), 1320 (m), 1301 (w), 1281 (s), 1236 (m), 1211 (w), 1183 (w), 1158 (w), 1124 (s), 1094 (w), 1071 (w), 1041(m), 999 (m), 948 (vs), 931 (vs), 887 (m), 836 (s), 778 (m), 727 (m), 713 (m), 671 (m), 660 (w), 534 (w), 498 (w), 464 (w), 422 (w) ESI + TOF: *m/z* 471.1788; error: 0.176026 ppm, DBE 5. Anal. Calcd for $C_{18}H_{32}PIr$: C, 45.84; H, 6.84. Found: C, 45.81; H, 7.54.

Acknowledgements

Financial support and scholarship from Conacyt (152280) and scholarship from ICyT DF (A.R.M.) are gratefully acknowledged. Thanks to M. Cervantes Vasquez, V. González Díaz, G. Cuellar Rivera and M. A. Leyva Ramirez for technical support in the IR, NMR, ESI + TOF MS and X-ray diffraction, respectively.

Appendix A. Supplementary data

Supplementary data to this article can be found online at https://doi.org/10.1016/j.jorganchem.2019.02.007.

References

[1] (a) G.J. Leigh, R.L. Richards, in: G. Wilkinson, F.G.A. Stone, E.W. Abel (Eds.), Comprehensive Organometallic Chemistry vol. 5, Pergamon Press, New York, 1982, pp. 599–603;
(b) J.D. Atwood, J.D., in: E.W. Abel, F.G.A. Stone, G. Wilkinson (Eds.), In Comprehensive Organometallic Chemistry II vol. 8, Pergamon, Oxford, 1995, pp. 365–400;
(c) J.M. O'Connor, In organometallic complexes of iridium, Sci. Synth. 1 (2002) 617–744.

[2] (a) G. Winkhaus, H. Singer, Chem. Ber. 99 (1966) 3610–3618;
(b) G. Pannetier, R. Bonnaire, P. Fougeroux, J. Less Common Met. 21 (1970) 437;
(c) A.L. Onderdelinden, A. van der Ent, Inorg. Chim. Acta 6 (1972) 420–426;
(d) J.L. Herde, J.C. Lambert, C.V. Senoff, Inorg. Synth. 15 (1974) 18–20;
(e) R.H. Crabtree, G.E. Morris, J. Organomet. Chem. 135 (1977) 395–403;
(f) R.H. Crabtree, J.M. Quirk, H. Felken, T. Fillebeen-Kahn, Synth. React. Inorg. Met. Org. Chem. 12 (1982) 407–413;
(g) D.R. Baghurst, D.M.P. Mingos, M.J. Watson, J. Organomet. Chem. 368 (1989) C43–C45;
(h) S.A. Bezman, P.H. Bird, A.R. Fraser, J.A. Osborn, Inorg. Chem. 19 (1980) 3755–3763.

[3] (a) M. Peruzzini, C. Bianchini, L. Gonsalvi, in: R.H. Crabtree, D.M.P. Mingos (Eds.), Comprehensive Organometallic Chemistry III vol. 7, Elsevier Ltd, Oxford, UK, 2007, pp. 319–324;
(b) I.I. Padilla-Martinez, M. Cervantes-Vásquez, M.A. Leyva-Ramirez, M.A. Paz-Sandoval, Organometallics 33 (2014) 6305–6318 (and references therein).

[4] (a) M. Martín, E. Sola, O. Torres, P. Plou, L.A. Oro, Organometallics 22 (2003) 5406–5417;
(b) S.M.W. Rahaman, J.-C. Daran, E. Manoury, R. Poli, J. Organomet. Chem. 829 (2017) 14–21;
(c) B. Cornils, W.A. Herrmann (Eds.), Applied Homogeneous Catalysis with Organometallic Compounds, VCH, Weinheim, 2002;
(d) P.A. Chaloner, M.A. Esteruelas, F. Joo, L.A. Oro, Homogeneous Hydrogenation, Springer-Science+Business Media, B. V., Dordrecht, 1994.

[5] P. Gamero-Melo, P.A. Melo-Trejo, M. Cervantes-Vasquez, N.P. Mendizabal-Navarro, B. Paz-Michel, T.I. Villar-Masetto, M.A. Gonzalez-Fuentes, M.A. Paz-Sandoval, Organometallics 31 (2012) 170–190.

[6] M.A. Paz-Sandoval, I.I. Rangel-Salas, Coord. Chem. Rev. 250 (2006) 1071–1106.

[7] J.R. Bleeke, Organometallics 24 (2005) 5190–5207.

[8] B.D. Murray, P.P. Power, Organometallics 3 (1984) 1199–1204.

[9] E.L. Muetterties, K.D. Tau, J.F. Kirner, T.V. Harris, J. Stark, M.R. Thompson, V.W. Day, Organometallics 1 (1982) 1562–1567.

[10] J.R. Bleeke, W.-J. Peng, Y.-F. Xie, M.Y. Chiang, Organometallics 9 (1990) 1113–1119.

[11] J.R. Bleeke, D. Boorsma, M.Y. Chiang, T.W. Clayton Jr., T. Haile, A.M. Beatty, Y.-F. Xie, Organometallics 10 (1991) 2391–2398.

[12] J.R. Bleeke, S.T. Luaders, Organometallics 14 (1995) 1667–1673.

[13] J.R. Bleeke, W.-J. Peng, Organometallics 6 (1987) 1576–1578.

[14] (a) R.D. Ernst, Chem. Rev. 88 (1988) 1255;
(b) R.D. Ernst, Comments Inorg. Chem. 21 (1999) 285–325.

[15] J. Müller, C. Schiller, P.E. Gaede, M. Kempf, Z. Anorg, Allg. Chem. 631 (2005) 38–46.

[16] A.K. Fazlur Rahman, M. Wilklow-Marnell, W.W. Brennessel, W.D. Jones, Acta Crystallogr. E73 (2017) 273–277.

[17] (a) D.A. Loginov, A.M. Miloserdov, Z.A. Starikova, P.V. Petrovskii, A.R. Kudinov, Mendeleev Commun. 22 (2012) 192–193;
(b) P.E. Gaede, C. van Wullen, Z. Anorg. Allg. Chem. 632 (2006) 541–552;
(c) K.V. Zherikova, N.B. Morozova, I.A. Baidina, J. Struct. Chem. 50 (2009) 570–573;
(d) D.V. Bonegardt, I.Y. Ilyin, T.S. Sukhikh, N.B. Morozova, Zh. Strukt. Khim. J. Struct. Chem. 58 (2017) 983–988.

[18] J.R. Bleeke, W.J. Peng, Organometallics 3 (1984) 1422–1426.

[19] (a) J.P. Collman, L.S. Hegedus, J.R. Norton, R.G. Finke, Principles and Applications of Organotransition Metal Chemistry, University Science Books: Mill Valley, CA, 1987, p. 70;
(b) J.R. Bleeke, A.J. Donaldson, Organometallics 5 (1986) 2402–2405;
(c) C. Li, M. Ogasawara, S.P. Nolan, K.G. Caulton, Organometallics 15 (1996) 4900–4903.

[20] Several experiments were carried out with a view to probe if in presence of excess of lithium pentadienide (3-8 equiv) the equilibrium mixture could be changed, affording the most favorable isomer. In all cases a mixture of **9a** and **9b** were observed through the ^{1}H NMR in a 2.0:1.0 ratio. Also, isolated crystals of **9b** showed in C_6D_6 the same equilibrium mixture of **9a** and **9b** in a 2.0:1.0 ratio. This mixture was heated at 65 °C for 12 h, with identical results.

[21] (a) B. Denise, G. Pannetier, J. Organomet. Chem. 148 (1978) 155–164;
(b) L.M. Haines, E. Singleton, J. Chem. Soc. Dalton (1972) 1891–1896.

[22] H.C. Volger, K. Vrieze, A.P. Praat, J. Organomet. Chem. 14 (1968) 429–440.

[23] R.H. Crabtree, S.M. Morehouse, Inorg. Chem. 21 (1982) 4210–4213.

[24] (a) H. Lebel, C. Ladjel, Organometallics 27 (2008) 2676–2678;
(b) E.P.K. Olsen, T. Singh, P. Harris, P.G. Andersson, R. Madsen, J. Am. Chem. Soc. 137 (2015) 834–842.

[25] The geometric parameter τ is applicable to five-coordinate structures as an index of the degree of trigonality, within the structural continuum between trigonal bipyramidal and rectangular pyramidal. For a perfectly tetragonal geometry is considered $\tau = 0$, while it becomes $\tau = 1$ for a perfectly trigonal-bipyramidal geometry. In the case of ideal SP geometry ($\tau = 0$) would have very similar Ir-mid-point cyclooctadiene olefinic distances as they would involve the same metal and ligand orbitals, while TBPY geometry ($\tau = 1$) would involve different orbitals, according to the preference of the cyclooctadiene olefinic bonds which could lay in an axial or an equatorial position.[26]

[26] A.W. Addison, T.N. Rao, J. Reedijk, J. van Rijn, G.C. Verschoor, J. Chem. Soc. Dalton Trans. (1984) 1349–1356.

[27] J.F. Frazier, J.S. Merola, Polyhedron 11 (1992) 2917–2927.

[28] (a) D. Seyferth, E.W. Goldman, J. Pornet, J. Oganomet. Chem. 208 (1981) 189;
(b) M.A. Paz-Sandoval, P. Powell, J. Organomet. Chem. 219 (1981) 81;
(c) M.E. Navarro-Clemente, P. Juarez-Saavedra, M. Cervantes-Vasquez, M.A. Paz-Sandoval, A.M. Arif, R.D. Ernst, Organometallics 21 (2002) 592–605.

[29] G.M. Sheldrick, Acta Crystallogr. A64 (2008) 112–122.

[30] Compounds **2** and **3** are quite volatile. The evaporation of the THF at low temperature required a long time, it was very slow, but it was necessary. When evaporation of the solvent was carried out at room temperature, as for example with compound **3**, the solution changed from yellow to green, avoiding the isolation of the product. In order to avoid decomposition of **3**, and to get compound **2** in good yield, the evaporation under reduced pressure at low temperature was accomplished.

[31] M. Burk, R. Crabtree, Inorg. Chem. 25 (1986) 931–932.

[32] B.A. Paz-Michel, F.J. González-Bravo, L.S. Hernandez-Muñoz, I.A. Guzei, M.A. Paz-Sandoval, Organometallics 29 (2010) 3694–3708.